

## ABSTRACT

Title of Document: INHIBITION OF PROTEIN-PROTEIN INTERACTIONS IN  
*MYCOBACTERIUM TUBERCULOSIS*

Paige Chan, Grace Chun, Elizabeth Corley, Isaac Jeong, Christopher Kim,  
Carolyn Lane, Ari Mandler, Nathaniel Nenortas, Michelle Nguyen, Ian Qian,  
Pradip Ramamurti, James Tuo, Jimmy Zhang

Directed by: Dr. Volker Briken  
Associate Professor, Department of Cell Biology and Molecular Genetics  
University of Maryland College Park

Tuberculosis is a highly contagious, infectious disease that kills about 1.8 million people annually. Current chemotherapeutic regimens are both inefficient and taxing to the patient. In addition, the disease has suboptimal treatment due to the rise of multidrug resistant strains of *Mycobacterium tuberculosis* (*Mtb*), the causative bacterial agent of tuberculosis. Therefore, we established a critical assay to identify novel drugs that interfere with specific *Mtb* virulence mechanisms. The mycobacterial protein fragment complementation (M-PFC) assay was developed to screen 725 compound drug panel to find candidate drugs that interfered with important virulence-causing protein interactions of *Mtb*. We targeted the EsxA-EsxB and EsxM-EsxN interactions of the type VII secretion systems of *Mtb*. Our screen identified 46 small molecules that inhibited both virulence interactions, exhibiting nonspecific activity against a model cell line *in vitro* as well as seven hits specific to one of the two cell lines. In the future, we hope to retest the seven unique positive hits to confirm their ability to inhibit specific protein-protein interactions of *Mtb*.

INHIBITION OF PROTEIN-PROTEIN INTERACTIONS IN *MYCOBACTERIUM*  
*TUBERCULOSIS*

By

Team MTB

Paige Chan, He (Grace) Chun, Elizabeth Corley, Isaac Jeong, Christopher Kim, Carolyn Lane,  
Ari Mandler, Nathaniel Nenortas, Michelle Nguyen, Ian Qian, Pradip Ramamurti, James Tuo,  
Jimmy Zhang

Thesis submitted in partial fulfillment of the requirements of the Gemstone Program  
University of Maryland, College Park 2017

Advisory Committee:

Dr. Volker Briken - Mentor & Associate Professor, Department of Cell Biology and Molecular  
Genetics  
University of Maryland, College Park

Dr. Kenneth Frauwirth - Lecturer, Department of Cell Biology and Molecular Genetics  
University of Maryland, College Park

Dr. Kevin McIver - Professor, Department of Cell Biology and Molecular Genetics  
University of Maryland, College Park

Dr. Patricia Shields - Senior Lecturer, Department of Cell Biology and Molecular Genetics  
University of Maryland, College Park

Dr. Daniel Stein - Professor, Department of Cell Biology and Molecular Genetics  
University of Maryland, College Park

© Copyright by

Paige Chan, He (Grace) Chun, Elizabeth Corley, Isaac Jeong, Christopher Kim, Carolyn Lane,  
Ari Mandler, Nathaniel Nenortas, Michelle Nguyen, Ian Qian, Pradip Ramamurti, James Tuo,  
Jimmy Zhang

2017

## **Acknowledgements**

We would like to thank our Gemstone mentor, Dr. Volker Briken, for supporting us, encouraging us, and guiding us through this process. Our team is extremely thankful for him and his entire research team for generously allowing us to use their lab space to conduct our research. We would also like to thank Dr. Jeffrey Quigley for his countless hours of support, guidance, and troubleshooting with our lab work. Our team would like to extend our gratitude to our librarians, Jeremy Garritano and Dr. Svetla Baykoucheva, who helped with our research, literature review, and writing process. Additionally, we would like to thank LAUNCH UMD, and all of our LAUNCH UMD donors, especially Michael Chan, Elizabeth Nenortas, Dennis Kim, Wenbin Tuo, Charu Murthy, Ming Zhang, and Xiufen Sui. The funding of our project would not have been possible without their support and generosity. We would like to thank the National Institutes of Health (NIH) for donating the 725 compound drug panel that was integral to our research. We would also like to acknowledge our Thesis Conference discussants, Dr. McIver, Dr. Frauwirth, Dr. Shields, and Dr. Stein for their time and interest in our research. Finally, we would like to thank the Gemstone Program for their continuous guidance and support, both through formal instruction and through advice and support given at all stages of this project. They provided invaluable words of wisdom and structure to keep our team on track and successful these past four years and our team could not be more thankful.

## Table of Contents

Acknowledgements.....	iv
Table of Contents.....	v
Table of Figures.....	vii
Table of Abbreviations.....	viii
Chapter 1: Literature Review.....	1
Epidemiology.....	1
Pathology.....	2
Current Treatments.....	4
Vaccine Treatment and History.....	4
Emergence of Multidrug Resistant Strains.....	5
Structure of the <i>Mtb</i> Cell Membrane.....	6
Type VII Secretion Systems.....	7
The ESX-1 Type VII Secretion System of <i>Mycobacteria</i> .....	9
The ESX-5 Type VII Secretion System of <i>Mycobacteria</i> .....	12
The PhoP and PhoR Two-component Regulatory System of <i>Mtb</i> .....	14
Repurposing Drugs for TB.....	16
Advantages of Using <i>Msm</i> as a Model System.....	17
M-PFC Assay.....	18
Alamar Blue.....	20
Chapter 2: Methodology.....	21
Bacteria and Culture Conditions.....	21
Cloning.....	22
Drug Screening to Determine Interference of Protein Interactions.....	27
Origin of the Compound Library Source.....	27
Growth Assay.....	28
Drug Screening Layout.....	29
Chapter 3: Results.....	31
Cloning Results.....	31
M-PFC Assay Drug Screening Results.....	34
Chapter 4: Discussion.....	37
Cefdinir and Ampicillin.....	37
Carmofur and 5-Fluorouracil.....	38
Mefloquine.....	38
2-Chloroadenosine.....	39
Meclizine.....	39
Proof of Concept.....	40
Limitations.....	40

Future Implications.....	41
Chapter 5: Conclusion.....	42
Appendix A.....	43
Appendix B.....	45
References.....	48

## Table of Figures

Figure 1. TB Incidence Map.....	2
Figure 2. <i>Mtb</i> Cell Envelope.....	7
Figure 3. Reconstitution of mDHFR in M-PFC System.....	19
Figure 4. Cloning Flowchart.....	23
Figure 5. Vector Maps of Empty Plasmids.....	25
Figure 6. PCR Primer Sequences.....	26
Figure 7. Restriction Enzymes.....	26
Figure 8. Colorimetric Plate Assay.....	29
Figure 9. Image of the Gel Containing the EsxA and EsxB Inserts.....	32
Figure 10. Growth assay for EsxAB <i>M. smegmatis</i> transformants.....	33
Figure 11. Growth assay for EsxMN <i>M. smegmatis</i> transformants.....	33
Figure 12. Table of All Unique Positive Results for Both the EsxAB and EsxMN Cell Lines...	34
Figure 13. Absorbance Data for Plate NCP004205 Tested Against the EsxMN Cell Line.....	35

### Table of Abbreviations

Terminology	Abbreviation
Alamar-Blue Trimethoprim	AB-TRIM
Bacille Calmette-Guerin	BCG
Biosafety Level 2	BSL-2
Centers of Disease Control and Prevention	CDC
Dimethyl sulfoxide	DMSO
Ethambutol	EMB
Human Immunodeficiency Virus	HIV
Isoniazid	INH
Murine dihydrofolate reductase	mDHFR
Multidrug-resistant TB	MDR-TB
Mycobacterial protein fragment complementation	M-PFC
<i>Mycobacterium smegmatis</i>	<i>Msm</i>
<i>Mycobacterium tuberculosis</i>	<i>Mtb</i>
National Institutes of Health	NIH
Optical Density	OD
PhoP-PhoR two- component system	PhoPR
Proline-glutamic acid	PE
Proline-proline glutamic acid	PPE
Pyrazinamide	PZA
Region of Difference 1	RD1
Rifampicin	RIF
Type VII Secretion Systems	T7SS
Tuberculosis	TB



Totally drug-resistant TB	TDR-TB
Trimethoprim	TRIM
Extensively drug-resistant TB	XDR-TB

## Chapter 1: Literature Review

### Epidemiology

Tuberculosis (TB) is a highly infectious, chronic airborne disease, that kills around 1.8 million people annually, falling under one of the top ten causes of death worldwide (“Global”, 2016). Despite current research and treatments, TB is the second leading cause of death in several regions, and one in three people carry the latent version of the disease worldwide. In 2015 alone, 10.4 million people fell ill with TB (“Global”, 2016). After infection, TB can be present in either the active or latent form. If the immune system cannot control TB growth, then TB is considered active. If it is controlled, then TB is latent. But according to Centers for Disease Control and Prevention, 5-10% of people with the latent form of TB will develop the active form of TB in their lifetime (“Reported”, 2007). TB is highly concentrated in certain areas of the globe in which six countries account for 60% of the total 10.4 million: India leads in this count followed by Indonesia, China, Nigeria, Pakistan and South Africa.

The probability of developing the disease is much higher for patients who are immunocompromised prior to their contact with tuberculosis, such as those infected with human immunodeficiency virus (HIV) as shown in **Figure 1**. Those infected with HIV are 20-30 times more likely to develop active TB; in 2013 alone, 360,000 people died from HIV associated TB (“Global”, 2016). Furthermore, the disease is highly contagious due to its mechanism of transmission. It is spread through aerosol transmission and primarily infects the pulmonary system. Aerosol droplets containing *Mycobacterium tuberculosis* (*Mtb*) enter the air passageways and travel through the respiratory tracts until they reach the alveoli of the lungs (“Reported”, 2007). Moreover, it is also possible for the bacteria to spread to other parts of the body; in extra-pulmonary tuberculosis, the causative agent disseminates to various organs

including the spine, kidneys, lymph glands, and gastrointestinal tract (“Global”, 2016; “Reported”, 2007).

### Estimated TB incidence rates, 2015

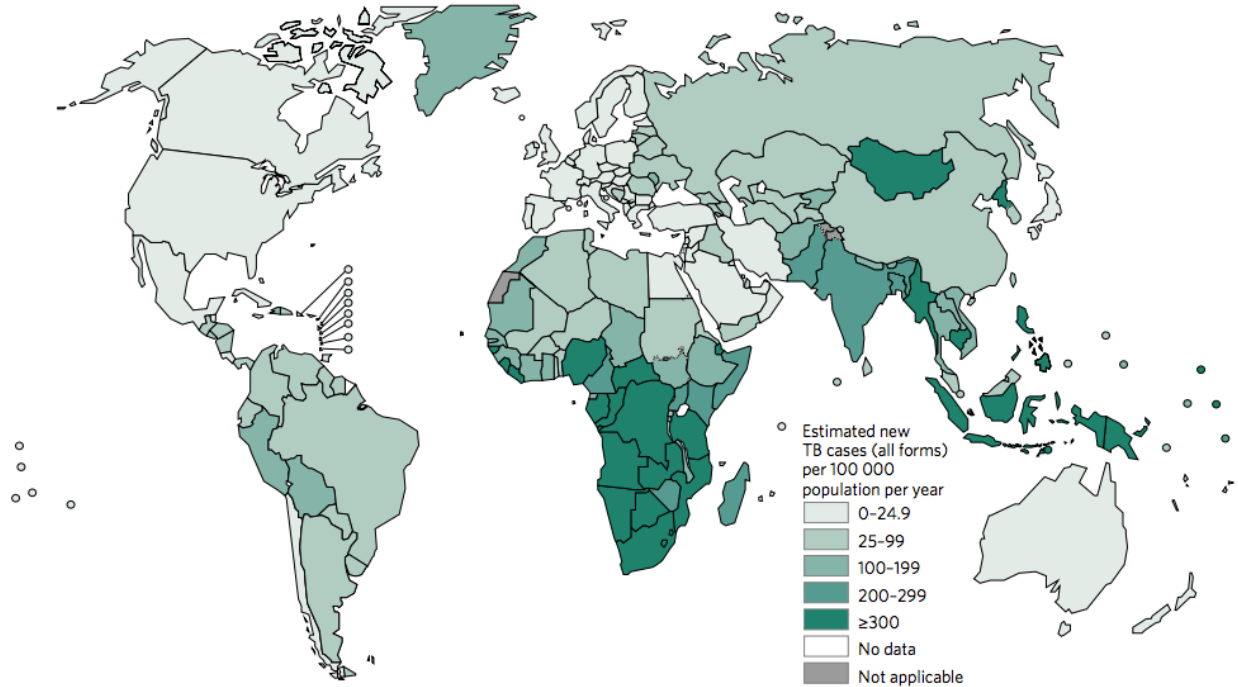


**Figure 1: TB Incidence Map.** Worldwide map depicting TB incidence rates in 2015 (“Global”, 2016).

### Pathology

TB begins as *Mtb*-containing aerosol droplets reach the alveolar surface of the lungs after inhalation (Schluger, 1988). The host immune system then recruits macrophages to phagocytize the *Mtb* bacilli. The bacilli cause endosomal manipulation, resulting in maturation arrest, lack of acid pH, and ineffective phagolysosome formation. In a normal immune response, once the bacilli is engulfed, the phagosomes will fuse with the lysosomes, forming the phagolysosome. The digestive enzymes originally contained in the lysosome will eventually kill the bacilli (Flynn & Chan, 2001). Ineffective formation of the phagolysosome thus results in unchecked bacillary proliferation. The macrophages then travel to the nearby lymph nodes and present the antigen to CD4 T-cells, also known as helper T-cells (Müller et al., 1987). This activates a cascade of

protein pathways that cause activation of macrophages, which results in chemokine secretions (Chan, 1999). These signaling molecules cause monocyte recruitment and ultimately a granuloma forms at the site of infection. The center of the granuloma formed due to *Mtb* is characteristically described as having a soft cheese-like appearance, also known as caseous necrosis. This is due to the deterioration of tissue in the center of a granuloma, where the bacilli are exterminated (Bean, 1999). Additionally, virulent strains of *Mtb* have ways to inhibit apoptosis of macrophages. The anti-apoptotic characteristics of the bacilli are a key factor for virulence as they permit further growth of the bacteria within the host (Abdallah et al., 2011). This results in a primary infection of *Mtb*, which leads to the formation of the primary complex or localized caseation. Progression can result in fibrosis and calcification in affected organs. Dissemination of the bacteria occurs through the host's blood and can affect either the lungs (pulmonary TB) or other organs (extrapulmonary TB).

Once the host recovers from the primary infection, a secondary infection may occur immediately or the bacteria may remain latent for an indefinite period of time. A secondary infection occurs if remnants of the bacteria persist in open lesions or if *Mtb* is reintroduced through aerosols into the host. Because the host's immune response is sensitized to *Mtb*, the tissue at the site of infection could experience caseating necrosis (Bean, 1999). Consequently, enough tissue in the lungs will erode so that the mycobacteria will spread throughout the airways, leading to a contaminated sputum and susceptibility for transmission (Smith, 2003). Additionally, *Mtb* can eventually gain access to both the pulmonary pathways from the heart as well as the systemic pathways, leading to lesions throughout the lungs and to additional organs. *Mtb* is well equipped to evade the adaptive immune response, so medicinal treatment is highly important for control of the disease (Kumar, Abbas, & Aster., 2012).

## **Current Treatments**

Current TB treatments are challenging for a variety of reasons. There is currently a four drug regimen prescribed for a period of 6-9 months that includes the administration of the first-line drugs: isoniazid (INH), rifampicin (RIF), pyrazinamide (PZA), and, ethambutol (EMB). Multidrug combination is important in TB treatment as each drug targets a different characteristic of TB virulence. These existing drugs and regimens are very enduring for infected patients because of their efficacy and time of therapy. Since the drugs must be able to penetrate human cells to reach the bacteria, which is actively designed to evading immune functions, the drugs are usually quite harsh on the human body. The regimen includes two months of intensive phase treatment and four to seven months of continuation phase treatment. The drug doses, long term treatment time frame, and economic cost of the 6-9 month intensive treatment make it especially difficult for individuals to overcome the disease (“Reported”, 2007).

## **Vaccine Treatment and History**

In 1943, Selman Waksman developed streptomycin, the first known effective antimicrobial agent (Farmer & Keshavjee, 2012). Although streptomycin has clear bactericidal effects on *Mtb*, some strains of the bacteria developed antibiotic resistance. This led to the development of two new antimicrobial agents, thiacetazone and para-aminosalicylic acid. These agents hold a synergistic effect with streptomycin that leads to more effective treatments and a decreased resistance to antibiotics. The current first-line drugs, INH, RIF, PZA, and EMB, are part of a 6-month regimen used to eradicate the bacteria (Kaufmann, 2013). Since 1990, TB incidence rates (the ratio of new cases of the disease to the total population) have not fluctuated considerably, which is especially evident in developing countries where there have been no improvements in reducing incidence rates of the disease (“Global”, 2016).

Currently, there is a safe, but limited vaccine called Bacille Calmette-Guerin (BCG), which was developed by Albert Calmette and Camille Guerin in the early 20th century (Kaufmann, 2013). This vaccine was first tested on a human subject in 1921 and still exists as the only licensed TB vaccine. It has been given to roughly 4 billion people worldwide to date, mainly to individuals living in countries with a high prevalence of TB. The CDC notes that the BCG vaccine is generally not recommended for use in the United States because of its rather low effectiveness against adult pulmonary TB, the rather low incidence levels and risk of infection in the US, and the vaccine's ability to interfere with the tuberculin skin test, the most common test to determine if an individual has TB ("BCG", 2017). It is mainly given to children in countries with a high risk of infection as the vaccine has been proven to be effective against disseminated TB, and is thus usually administered soon after birth (Farmer & Keshavjee, 2012). However, it has been found that BCG provides insufficient protection against the disease in adults, rendering the need for newer, more efficient treatments. It does not prevent against reactivation of latent pulmonary infection into the active form, nor does it protect against primary infection ("Global", 2017). Consequently, much of the efforts in the US to prevent and control the spread of TB is concentrated on the early detection and treatment of infected individuals with active TB, in addition to preventive therapy for those with latent TB in order to minimize and prevent the progression to its infectious active form. In terms of the reactivity of the BCG vaccine to the tuberculin skin test, it has the potential to induce a false positive result in vaccinated individuals ("BCG", 2017).

### **Emergence of Multidrug Resistant Strains**

The TB epidemic is magnified by the emergence of multidrug resistant strains, that result from the failure to adhere to long term treatment ("Global", 2016). Multidrug Resistant

Tuberculosis (MDR-TB) is resistant to INH and RIF and thus require a combination of second line drugs, aminoglycosides and fluoroquinolones (Dietrich & Doherty, 2009). The treatment is more complicated as it is more expensive and lasts approximately 8 months. Currently, MDR-TB has spread to an estimated half-million cases worldwide. Extensively drug-resistant tuberculosis (XDR-TB) is resistant to INH, RIF, aminoglycosides, fluoroquinolones, and either amikacin, kanamycin, or capreomycin. These patients are left with limited treatment options and are at most risk. Currently, XDR-TB has been found in more than 84 countries, which is extremely concerning due to its high risk (Zumla, Nahid, & Cole, 2013). The duration, adverse side effects, financial burden of current treatment and emergence of highly resistant *Mtb* strains calls for new drugs that provide both reduced toxicity and increased attenuating abilities.

### **Structure of the *Mtb* Cell Membrane**

Mycobacteria possess a complex cellular envelope, consisting of several critical layers that contribute to its resistance to host cell defense mechanisms as shown in **Figure 2**. In comparison to gram-negative bacteria, gram-positive bacteria are generally considered more simple in terms of structure (Abdallah et al., 2007). Generally, the cellular envelope of a mycobacterium consists of a complex mycomembrane surrounding an inner membrane with an outer capsular layer. The mycomembrane is characterized by the presence of hydroxylated branched-chain fatty acids called mycolic acids that are covalently bonded to the cell-wall matrix, forming a low fluidity, hydrophobic layer (Abdallah et al., 2007). These mycolic acids are covalently intercalated with peptidoglycan and arabinogalactan. The outer capsular layer is characterized by the presence of different, non-covalently linked free lipids and proteins such as sulphatides, phenolic glycolipids, phthiocerol dimycocerosates, dimycolyltrehalose, and phosphatidylinositol mannosides that are specific to mycobacteria (Walters et al., 2006). The

combination of these layers all serve as protective barriers for survival in host phagosomes due to an increased tolerance to protective host factors such as antimicrobial peptides and oxidative radicals (Ates et al., 2015). In order for *Mtb* to exhibit its virulence, it uses a type VII secretion system (T7SS) to export proteins across the physical layers (Solomonson et al., 2015).

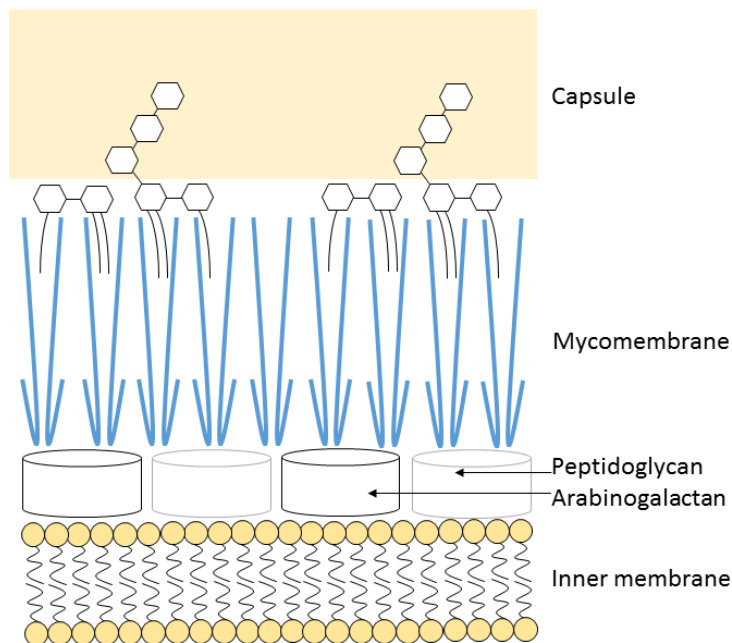


**Figure 2: *Mtb* Cell Envelope.** Structure of the cell envelope of *Mycobacterium tuberculosis*

### Type VII Secretion Systems (T7SS)

All mycobacterial species use T7SS to secrete proteins across their hydrophobic, impermeable cell envelope (Abdallah et al., 2007; Houben et al., 2014). Moreover, pathogenic mycobacteria require the T7SS to transport virulence factors through their protective and unique cell membranes into infected host cells (Daleke et al., 2012). Pathogenic mycobacteria such as *Mtb* form a unique order of bacteria called *Corynebacteriales* characterized by the presence of mycolic acids within their cell wall (Houben et al., 2014). *Corynebacteriales* tend to be strong, resilient organisms due to their protective outer membrane (Houben et al., 2014). This protective membrane restricts protein transport and is one of the main reasons why pathogenic



mycobacteria require T7SS (Houben et al., 2014). Once T7SS substrates are recognized in the cytosol, it is thought that they are targeted to the inner membrane and transported over the mycobacterial cell envelope (Houben et al., 2014). This transport is partially mediated by T7SS membrane components that form a translocation channel (Houben et al., 2014). There are still many unknowns about T7SS, including the method of substrate recognition, but it is known that substrates are normally secreted as folded dimers and have similar bundles of 4 alpha-helices followed by a secretion motif (Houben et al., 2014).

Up to five of these T7SS can be encoded within the mycobacterial genome, with the number of genes and overall size of the loci varying significantly (Abdallah et al., 2007; Houben et al., 2014). The five systems are named ESX-1 through ESX-5, in which three have been shown to be essential for virulence and viability of pathogenic species (Houben et al., 2014). The three loci, ESX-1, ESX-3, and ESX-5, are involved in the secretion of proteins while ESX-2 and ESX-4 are not known to be integral systems as neither have been proven to show active secretion of substrates (Houben et al., 2014).

The first of the T7SS to be discovered was ESX-1 in *Mtb* (Stanley, 2003). The existence of the ESX-1 system was first evidenced in an experiment when the *Mycobacterium bovis* BCG vaccine for tuberculosis was complemented with the region of difference 1 (RD1) locus on *Mtb* (Abdallah et al., 2007). When ESX-1 was discovered, it was shown to allow the secretion of two small culture filtrate proteins, originally called ESAT-6 and CFP-10 and now known as EsxA and EsxB, respectively (Houben et al., 2014). The proline-glutamic acid (PE) and proline-proline glutamic acid (PPE) proteins, which have been consistently associated with the ESX systems, are secreted by the ESX-1 and ESX-5 systems (Abdallah et al., 2007, Daleke et al., 2012). The PE and PPE proteins are structurally similar to the proteins EsxA and EsxB, containing the four-

helix bundle in antiparallel fashion, and have a similar genetic organization (Houben et al., 2014). For the purposes of our study, we are focusing on ESX-1 and ESX-5 systems for their vital roles in the virulence of *Mtb* (Abdallah et al., 2007; Bottai et al., 2012; Houben et al., 2014). Inhibition of these two systems is predicted to result in an attenuated phenotype of *Mtb*.

### **The ESX-1 Type VII Secretion System of *Mycobacteria***

The genes for the T7SS ESX-1 are located on the *Mtb* genome at the RD1 locus (Guinn et al., 2004). RD1 is important for the virulence of *Mtb* as several mutants lacking this region, including BCG, experience attenuation *in vitro* and *in vivo* (Guinn et al., 2004). In addition to coding for the ESX-1 secretion system, RD1 codes for secreted factors important for virulence (Guinn et al., 2004; Pym et al., 2002).

To understand the role ESX-1 system plays in virulence it is important to understand its functions and what exactly is being secreted by the system. As previously stated, two of the proteins secreted by the ESX-1 system are the 6 kDa secreted antigen target, EsxA, and the 10 kDa culture filtrate protein, EsxB (Simeone et al., 2009). Through many experiments EsxA and EsxB were found to be key virulence factors (Abdallah et al., 2007; Brodin et al., 2005; Simeone et al., 2009).

Wirth *et al.* in 2012 gave insights into the intracellular location of the ESX-1 system by fluorescently tagging the protein Rv3871 and examined its location in the cell in *Msm*. The protein was found to move to a distinct cell pole where there was a singular signal (Wirth et al., 2012). The researchers used a different species of mycobacteria, but their results do give us insight into the possible location of the complex in *Mtb*, as well as a potential screening method that could identify attenuation (Wirth et al., 2012). Looking closer at the two main proteins secreted by the ESX-1 system, EsxA is a member of the WXG100 family of proteins that are

characterized by being approximately 100 amino acids in length and having tryptophan-variable residue-glycine as a conserved amino acid sequence (Brodin et al., 2005). EsxA and EsxB form a tight 1:1 heterodimeric complex, which is then secreted by *Mtb* through recognition of the C-terminus on EsxB by ESX-1 (Brodin et al., 2005; Lou et al., 2017). Secretion of this complex is also dependent on EspA, EspC, and EspD (Stoop et al., 2012). It should be noted that while other proteins known to be involved in the structure of ESX-1 localize to the cell pole, EsxA and EsxB does not localize to the cell pole with structural components (Wirth et al., 2012).

More recently it has been found that the major virulence factors, EsxA and EsxB, are co-secreted with two other factors, EspA and EspC (Lou et al., 2017). Lou and colleagues (2017) found that EspC and EsxA associate in the cytoplasm and membrane, then EspC polymerizes during secretion from *Mtb*. They concluded that EspC is either a component of the secretion system or has some effect on the function of ESX-1. While the steps of ESX-1 secretion and the structure of the secretory apparatus are still unknown, it is known that most T7SS substrates carry a YxxxD motif as a general secretion signal (Daleke, et al., 2012; Lou et al., 2017). EspC is one of these substrates, a small protein with a YxxxD motif. Taking this into account with EspC's co-secretion with EsxA, it is likely that the two proteins form a complex during translocation (Lou et al., 2017). During secretion, EspC polymerizes into a filamentous structure that seems to span the capsule of *Mtb* and might represent a "secretion needle" of the ESX-1 system (Ates & Brosch, 2016; Lou et al., 2017).

Two other components of the ESX-1 structure are the soluble proteins EccB and EccD, and there have been recent discoveries in the structure of each (Wagner et al., 2016). EccB consists of a central domain and four repeat domains that form a 2-fold symmetrical structure. The repeating domains may play a role in anchoring the ESX-1 system due to their

similarity to a known binding protein (Wagner et al., 2016). EccD<sub>1</sub>, a cytoplasmic protein, has a “ubiquitin-like” fold and forms a dimer. Knowing the structure to these ESX-1 components may help uncover ways to disrupt *Mtb* virulence in the future and would be vital to tuberculosis intervention strategies (Wagner et al., 2016).

While investigating the mechanism of EsxA, Simeone and colleagues (2012) showed that *Mtb* lacking RD1 are confined to the phagosome. When transfected with RD1 on a plasmid, BCG (BCG::RD1) was able to escape host phagosomes and move into the cytosol (Simeone et al., 2012). This BCG mutant was successfully contained in host phagosomes when the *esxA* gene was knocked out of the bacterial chromosome, which indicates that EsxA is vital for the bacteria to escape into the cytosol (Simeone et al., 2012). After gaining access to the host cytosol, *Mtb* and BCG::RD1 proliferated unhindered within the macrophage and cause subsequent host cell necrosis. Necrosis is not ideal for the host as it allows for the rapid proliferation of virulent bacteria whereas programmed macrophage death does not allow for the same levels of *Mtb* proliferation (Simeone et al., 2012).

It has been demonstrated that ESX-1 is vital for the virulence of *Mtb* and strains, such as BCG, that lack the presence of RD1 do not express the same virulence (Guinn et al., 2004). Virulence is conferred by the EsxAB complex, which is targeted and secreted by ESX-1 (Brodin et al., 2005). Secretion of EsxA allowed for *Mtb* phagosome escape and cause subsequent host cytotoxicity (Simeone et al., 2012). For these reasons, the ESX-1 secretion system and its substrates are viable drug targets.

## The ESX-5 Type VII Secretion System of Mycobacteria.

In contrast to ESX-1, ESX-5 is most recently evolved and restricted to slow-growing mycobacteria. This group of mycobacteria includes the major pathogenic species *Mtb*, *Mycobacterium leprae*, *Mycobacterium ulceran*, and *Mycobacterium marinum* (*Mm*) (Gey van Pittius et al., 2006). While ESX-5 has similar gene composition in comparison to the other T7SSs, it has functional variation. Generally, it is responsible for cell wall integrity and stability, host cell lysis and strong attenuation, using a duplicated four-gene region (ESX-5a) to transport secretory proteins and virulence factors (Shah & Briken, 2016).

The ESX-5 T7SS is regulated at the transcriptional level by the Pst/Sen X3-RegX3 system (Elliott and Tischler, 2016). Under phosphate-limiting conditions, the ESX-5 system becomes activated in response to this environmental stimulus and its mechanism is RegX3 independent (Elliott & Tischler, 2016). Within the ESX-5 locus, there is a pair of *esx* genes that code for the EsxM and EsxN proteins, which dimerize in *Mtb* (EsxMN), are antigens found to induce CD4<sup>+</sup> T-cell responses in various animal and human models. Upstream from the *esxN* gene, the *ppe25-pe19* genes, named for their motifs near the N-terminus, code for associated PE and PPE proteins. The ESX-5 system is largely responsible for the secretion of these highly immunogenic, virulence-associated proteins, whose genes are found in slow-growing bacteria such as *Mtb*, coded by about 9% of its genome (Abdallah et al., 2007). This family of proteins is associated with virulence and cell wall integrity (Bottai et al., 2012). The ESX *ecc* (*esx* conserved components) genes surrounding the *ppe-pe-esx* genes encode supporting membrane proteins involved in ATP-binding that contribute to the export of Esx proteins (Di Luca et al., 2012).

The functionality of the ESX-5 T7SS has been studied in various mycobacterial species. In *Mm*, the ESX-5 system plays a critical role in the modulation of cytokine responses by macrophages (Abdallah et al., 2008). The use of an ESX-5 knockout in *Mm* did not induce inflammasome activation or IL-1 $\beta$  secretion, indicating that ESX-5 is essential to these processes (Abdallah et al., 2011). While the ESX-5 secreted proteins are not required for the translocation of *Mtb* or *Mm* into host cells, the system does induce a caspase-independent cell death after translocation occurs, allowing infection of other cells (Abdallah et al., 2011). In a more recent study, the ESX-5 T7SS was found to play a substantial role in cell wall integrity, more specifically in the stability in the capsule layer of the cell wall. In *Mm*, ESX-5 and PPE10 knockouts compromised the integrity of the capsular layer, which contains the substrates of the T7SS, and also leads to reduced surface hydrophobicity (Ates et al., 2016). In ESX-5 knockouts, PPE10 has been identified as the substrate responsible for the deficiency in the surface localized proteins of the capsular layer of pathogenic mycobacteria, in addition to morphological differences (Ates et al., 2016). In infected strains of Zebrafish, while ESX-5 mutant *Mm* led to slight attenuation in embryos, it also indicated highly increased virulence in infected adults, as seen by early granuloma formation and an increase in proinflammatory cytokines (Weerdenburg, 2012). Additionally, studies have indicated that the ESX-5 system is also largely responsible for the uptake and use of hydrophobic carbon sources (Ates et al., 2015).

To determine the role of the ESX-5 system in *Mtb*, the selected ESX-5 genes in the *Mtb* H37Rv strain, *eccD*, *eccA*, *rv1794*, *esxM* and *ppe25-pe19*, were inactivated with mutants, knocking out factors individually (Bottai et al., 2012). To determine the ability of the mutants to secrete EsxN in order to export PE/PPE proteins, the mutants were tested in vitro. To determine their effect on virulence, the ESX-5 mutants were tested in ex vivo and in vivo, using immune-

deficient mice. While the deletion of *rv1794* showed no significant difference from wild type secretion levels, the remaining four mutants relay strong defects in secretion of EsxN and the small hydrophilic PE/PPE protein, PPE41. PE and PPE proteins rely on the secretion of LipY, a substrate of the ESX-5 system in *Mm* (Daleke et al., 2011). PE and PPE proteins thus have a multitude of roles in virulence, both for its membrane structure and for its ability to attack the host. The immunogenicity of the PE and PPE proteins have been found to relay back to EccD<sub>5</sub> regulation (Sayes et al., 2012). Though the various ESX secretion systems do not complement each other, both ESX-1 and ESX-5 play significant roles in cell-to-cell migration and macrophage escape, suggesting that both T7SS operate independently in the cellular infection cycle (Abdallah et al., 2007).

### **The PhoP and PhoR Two-component Regulatory System of *Mtb***

The PhoP-PhoR (PhoPR) system is a two-component regulatory signal transduction system. Bacterial adaptation to host responses usually take the form of transcriptional activation of genes, whose products specifically help the bacterium live and cope with the surrounding environment. The two-component system contains an environmentally responsive histidine kinase and a response regulator, that is activated by the cognate histidine kinase. The aspect of the two component system plays a major role in the bacterial responses to altered environments (Stock et al., 2000). Therefore, this regulatory system of *Mtb* allows it to function and survive in harsh host cell environments, as well as evade the host cell response.

In *Mtb*, this specific system controls around two percent of the genome and is thought to play a significant role in bacterial pathogenesis (Santos-Beneit, 2015). The importance of the system for *Mtb* survival is based on the production of complex lipids which play an essential role in creating the cell envelope for the bacterium. More than half of the genes that the system

regulates are annotated to encode proteins involved in lipid metabolism and secretion in addition to the creation of the components necessary for the cell envelope.

Through knockout studies, the importance of the PhoPR system was established, where PhoP was inactivated in the *Mtb* strain H37Rv. Disruption of the system caused a marked attenuation of growth in macrophages and mice, establishing the importance of the presence of the system for growth of the bacterium. Strains where the two component system was inactivated made the bacterium more susceptible to a low magnesium environment, prohibiting the bacterium from proliferating and growing in such an environment. The PhoPR system is also essential for the biosynthesis of sulphatides and trehaloses. The cells from the knockout study did not contain these important complex lipid components of the cell envelope. Disruption of the genes that encoded the PhoPR two component system produced cells lacking in the complex lipids, making it more susceptible to host cell defense mechanisms (Walters et al., 2006).

The genes that were regulated in generating these complex lipids were found to be *pks2* and *msl3*, encoding enzymes for the biosynthesis of sulphatides and trehaloses. In the cells with the mutated *phoP* gene, there was reduced expression and transcription of *pks2* and *msl3*, and therefore subsequent reduced production of the complex lipids. The cell envelope of the PhoP mutant lacked trehaloses and methyl branched fatty acids. The absence of these complex lipids could potentially compromise the permeability of the cell envelope, and lead to exposure of proteins normally protected by the *Mtb* capsule, and creating a greater sensitivity to the host cell response. PhoP also positively regulates two other genes involved in lipid metabolism, *fbpA* and *lipF* (Walters et al., 2006). Both of these genes have been speculated to function in generating lipases. These lipases have been thought to degrade host lipids during infection, making fatty acids available as building blocks for lipid biosynthesis for the bacterium (Walters et al., 2006).



While the necessity of the two component system for creation and generation of the complex lipids was established, the necessity of a high magnesium environment when the mutant was introduced was still left undetermined. The researchers found that the *Mtb phoP* mutant required high levels of magnesium when the *phoP* gene was disturbed (Walters et al., 2006). While the researchers were able to state that the *Mtb* PhoPR system does not respond in sensing magnesium starvation, they hypothesized that the requirement of the mutant for high levels of magnesium could be a direct consequence of the structural alterations of the cell envelope. The absence of the sulphatides and trehalose components in the mutant may impair the integrity of the cell wall. Therefore, without these components, magnesium can function to stabilize the cell wall. When these components were missing in the mutant, high levels of magnesium fostered growth for the cells, whereas low levels of magnesium hindered proliferation (Walters et al., 2006).

Without these components, the integrity of the bacterium as a whole becomes compromised, and the cell becomes more susceptible to the host cell defense mechanisms. Thus, PhoPR is important for virulence and the disruption of this interaction should produce an attenuated strain of *Mtb* (Ryndak et al., 2008).

### **Repurposing Drugs for TB**

The long duration, high expense, high toxicity, and rise of MDR-TB and XDR-TB associated with current TB treatment brings to light the need for novel therapeutic drugs which can attenuate the disease in a stronger and more timely way (Zumla, Nahid, & Cole, 2013). Repurposed drugs offer a unique solution to the long-term and resource draining process that currently exists for drug approval (“Reported”, 2007). Today, a notable amount of drugs have

been repurposed for TB treatment: clofazimine, a drug previously used for leprosy, has been recently found to treat TB in mouse models (Verma et al., 2013).

Repurposing drugs that were used for other causes previously and show usefulness in treating tuberculosis allows researchers to bypass the lengthy average of 12 years for discovery, preclinical development, and clinical development for FDA approval (“Reported”, 2007). Non-conventional drug targets may also affect *Mtb* virulence systems that were not previously considered and thus provide insight to new methods of disruption. Current anti-TB drugs target central processes of the organism; however, administering repurposed drugs to possibly disrupt peripheral routes of virulence may be more efficient in eradicating the organism. Because virulence pathways are not targeted by anti-TB drugs, these pathways are currently not under survival pressures to mutate, so their vulnerability can be targeted for new treatments. Furthermore, in order to be of wide use, novel drugs should be compatible with current antiretroviral drugs used for HIV-AIDs patients, and this is more easily screened for when testing well established drugs. For this reason, NIH has created a Molecular Libraries Initiative which contains Molecular Libraries Small Molecule Repository for researchers to test the repurposing of clinically approved drugs.

### **Advantages of Using *Msm* as a Model System**

The model organism chosen for our project was *Msm*. *Mtb* and *Msm* both come from the *Mycobacterium* genus. This homology allows for *Mtb* and *Msm* to share important characteristics such as biosynthetic pathways and cell membrane type (Tortoli, 2014). Conversely, it also allows for important differences to exist; most notably, *Msm* replicates more quickly and transforms more efficiently than *Mtb* (Michod, Bernstein, & Nedelcu, 2008). Most importantly, *Msm* allows for safer handling -- requiring Biosafety Level 2 (BSL-2) labs as opposed to *Mtb*, which requires

Biosafety Level 3 (BSL-3) labs (Singh et al., 2006). This is primarily due to the non-pathogenic nature of *Msm* in humans (Bohsali et al., 2010). These factors encouraged the selection of *Msm* as an optimal model system and carrier of relevant *Mtb* protein pairs.

### **M-PFC Assay**

In this study, we sought to test a panel of repurposed drugs in disrupting important virulence interactions within the cell, namely type VII secretion systems and two-component regulatory signal transduction system, although testing for the latter system ended prematurely due to issues assembling the necessary assay for that system. In order to measure drug interaction, we required to use an assay that would give a clear indication of protein-protein interaction inhibition. The M-PFC assay was specifically designed to detect cytoplasmic and membrane-bound protein interactions within mycobacterium cells. In the assay, two proteins with known interactions *in vivo* were attached to mDHFR reporter fragments [F1,2] (expressed in pUAB300) and [F3] (expressed in pUAB400) as depicted in **Figure 3**. If [F1,2] and [F3] reassembled to a functional mDHFR, it conferred resistance against the antibiotic trimethoprim (TRIM) by allowing the bacteria to digest the antibiotic. [F1,2,3] refers to the polypeptide domains of the full enzyme mDHFR. There are several advantages of using the M-PFC assay, including its ability to detect a diverse range of protein-protein interactions. In previous tests, the M-PFC assay was successful in identifying interactions among proteins originating from *Mtb* (Bansal et al., 2017). Although this system can detect a diverse range of protein-protein interactions, it only attains a positive result, or successful coupling, between specific proteins that are known to have interactions (Singh et al., 2006).

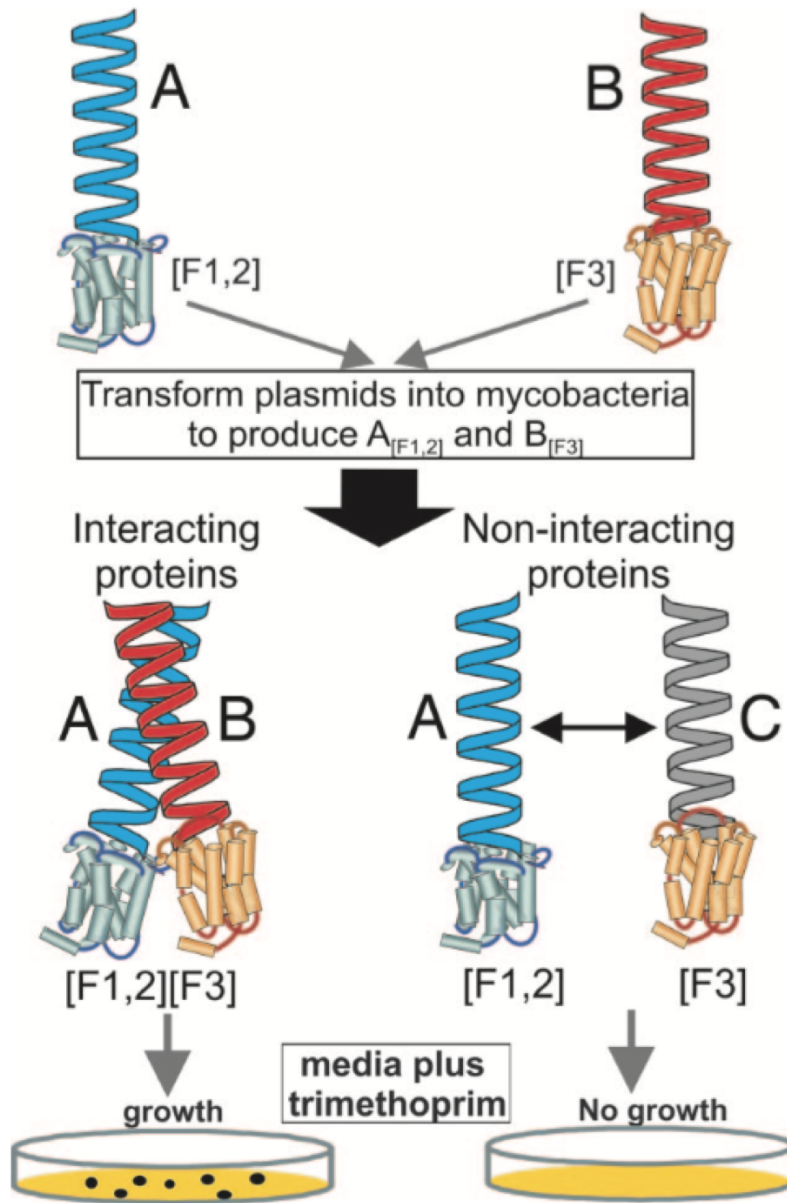


**Figure 3: Reconstitution of mDHFR in M-PFC System.** Diagram depicting the reconstitution of mDHFR in the survival-based assay. Interacting proteins A&B allow for assembly of a functional mDHFR and, as a consequence, confer antibiotic resistance in the presence of TRIM. Non-interacting proteins A&C do not allow for mDHFR reconstitution and therefore prevent cellular growth (Singh et al., 2006).

## **Alamar Blue**

Reconstitution of mDHFR due to protein-protein interactions was simply monitored via survival-based assay. The M-PFC provides in-depth analyses about mechanisms such as protein modifications on protein-protein associations. Hence, the readout for in-depth analysis, named AB-TRIM, incorporates Alamar Blue. This compound has been used previously to assess the viability of mycobacteria in the presence of antimycobacterial compounds in 96-well formats. AB-TRIM is a colorimetric plate assay. The color of AB transitions from blue to pink at OD560 depending on the level of growth, which is heavily dependent on the degree of reconstitution of mDHFR. Alamar Blue was the primary method of quantification of protein-protein interaction in *Msm*. Protein-protein interaction led to the reconstitution of the mDHFR, which led to the digestion of TRIM that allows for cell proliferation. The lack of protein-protein interaction meant that the mDHFR was nonfunctional and the cells died (Singh et al., 2006).

## Chapter 2: Methodology

The first step in analyzing the efficacy of the NIH drug panel on the model *Msm* mc<sup>2</sup> 155 cell line involved cloning our genes of interest, which code for dimer-forming proteins, onto plasmids for use in the M-PFC assay. Using the assay, we evaluated protein-protein interactions within *Msm* in the presence of unique drugs through cellular growth levels. Quantification of our results was obtained through spectroscopy with Alamar Blue.

### Bacteria and Culture Conditions

We transformed the DH5a strain of *E. coli* using pUAB300 and pUAB400 plasmids (Appendix A), which were then selected for on LB plates containing Hygromycin (final concentration of 50 µg/mL) or Kanamycin (final concentration of 150 µg/mL), respectively. These plasmids conferred resistance to their respective antibiotic, and colony growth was observed after overnight incubation at 37°C. Isolated colonies were subsequently picked and overnight liquid cultures were made with 3 mL of LB broth and either 3 µL of Kanamycin (50 mg/mL stock) or 9 µL of Hygromycin (50 mg/mL stock). Frozen glycerol stocks of culture were made containing 15% glycerol (Mai et al., 2011; Singh et al., 2006).

Following successful attainment of transformed *E. coli*, the plasmids were transferred to create *Msm* recombinant cells. *Msm* cells were initially grown in 7H9 medium with 10% Albumin Dextrose Catalase (ADC), 0.5% glycerol, and 0.05% Tween-80. The 7H9 medium was then supplemented with either 3µL Kanamycin (50 mg/mL stock) or 9µL of Hygromycin (50 mg/mL stock). Similar to the *E. coli* protocol, the antibiotics in the media are specific to the transformed plasmids -- pUAB300 and 400 -- conferring selective resistance. The *Msm* cells were cultured to a target optical density of 600 (OD600) range of 0.5-1.0, which remained within the exponential growth phase. They were subsequently frozen at -80°C in 20% glycerol. The

cells were then thawed and incubated overnight in 7H9 broth without antibiotic present. The cells were diluted to target concentrations for the following assay (Mai et al., 2011; Singh et al., 2006).

In preparation for the M-PFC assay, 7H9 media containing Kanamycin or Hygromycin was supplemented with 50 µg/mL TRIM. Initially, cell concentrations in TRIM supplemented 7H9 media were low during assays. To resolve this issue, overnights of transformed mc<sup>2</sup> 155 cells were grown in TRIM supplemented 7H9 media to concentrate the amount of transformed cells in the frozen stocks (Mai et al., 2011; Singh et al., 2006).

## **Cloning**

### **Constructing Desired Fusion Proteins for the M-PFC Assay to Test for Protein-Protein Interaction**

In order to perform the M-PFC assay, the pair of proteins suspected to interact will have to be expressed as a fusion protein with the murine dihydrofolate reductase (mDHFR) domains. This required each gene of a suspect protein, or insert, to be incorporated into a plasmid that held the gene for one of the mDHFR domains. After each insert was incorporated into its corresponding plasmid, both fusion plasmids expressing the interacting pair of proteins were transformed into our *Msm* cell line. In doing so, the *Msm* cell line had the ability to produce desired proteins, which were necessary for completion of our M-PFC assay.

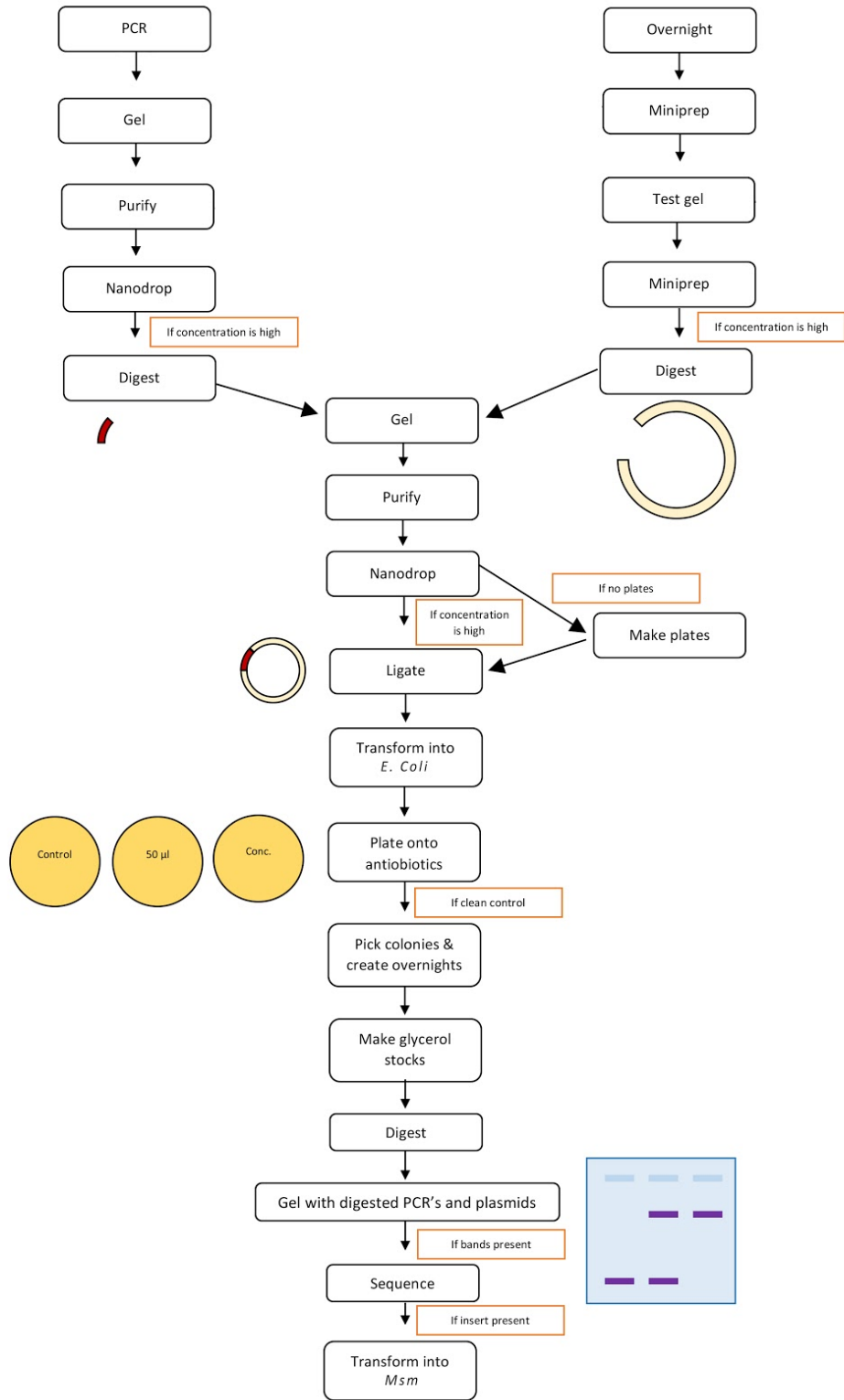


**Figure 4: Cloning Flowchart.** Flowchart depicting the sequence of cloning and transformation in creation of *Msm* recombinant cells.



To create these fusion plasmids displayed in **Figure 5**, the cloning method outlined in **Figure 4** was employed. The inserts for *esxA*, *esxB*, *esxM*, *esxN*, *phoP*, and *phoR* were obtained through PCR. The forward and reverse primers for each insert are listed in **Figure 6**. Annealing temperatures for *esxA&B* and *esxM&N* were 56°C, while the annealing temperature was 58°C for *phoP&R*. These inserts were then digested with the appropriate pairs of restriction enzymes listed in **Figure 8** that would allow fusion with the appropriate plasmid. The M-PFC plasmids that contained the mDHFR domains, pUAB300 and pUAB400, were likewise digested with specific pairs of restriction enzymes to correspond with the given inserts. The pair of restriction enzymes created two unique sticky ends in the multiple cloning site of the circular M-PFC plasmid to form a linear plasmid. The inserts and plasmids of interest were isolated with gel electrophoresis by cutting the appropriate bands. The inserts were incorporated into the linear M-PFC plasmid by treating the two parts with ligase (New England BioLab Inc., 2014). The inserts and vectors were ligated according to the following pairs: *esxA* with pUAB300, *esxB* with pUAB400, *esxM* with pUAB300, *esxN* with pUAB400, *phoP* with pUAB300, and *phoR* with pUAB400. The linear plasmids were treated with phosphatase to prevent self-ligations; phosphatase activity was then terminated during clean up (New England BioLab Inc., 2014).

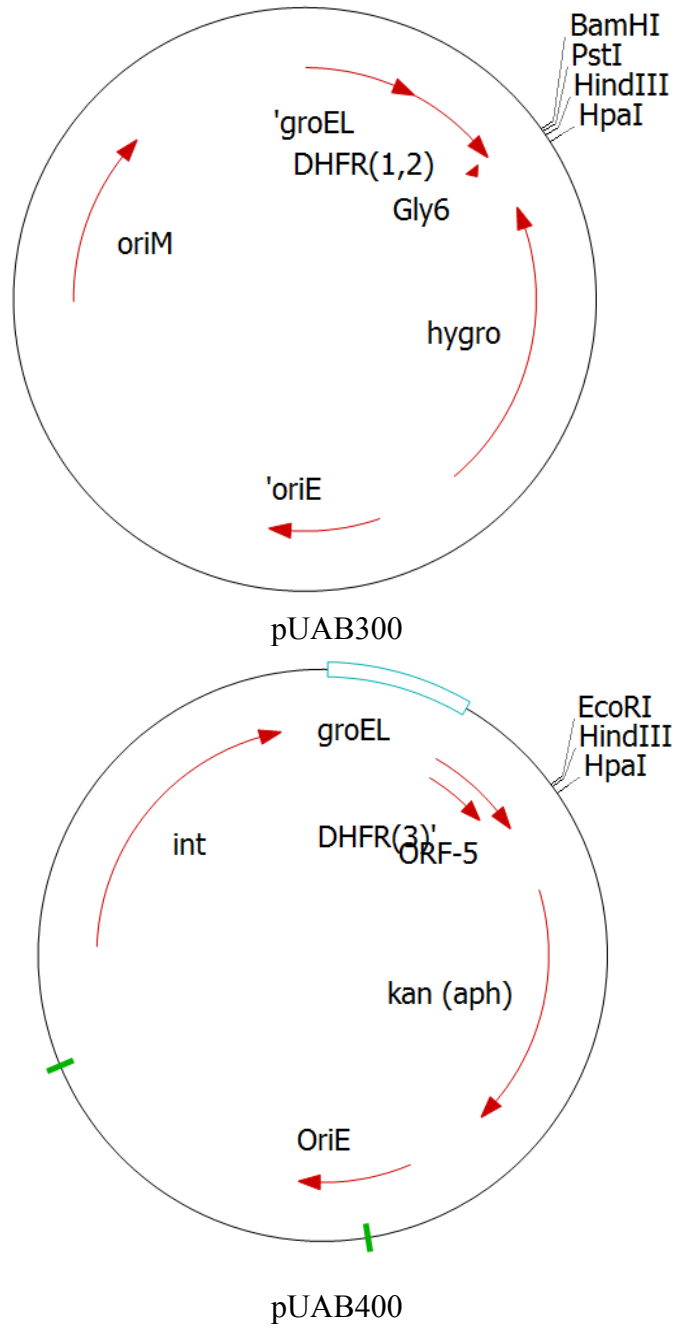


**Figure 5: Vector Maps of Empty Plasmids** a) pUAB300 and b) pUAB400, with corresponding restriction sites (BamHI, PstI, HindIII, and HpaI for pUAB300; EcoRI, HindIII, and HpaI for pUAB400), antibiotic resistant genes (hygromycin for pUAB300; kanamycin for pUAB400), and fusion proteins (DHFR(1,2) for pUAB300; DHFR(3)' for pUAB400).

Gene	Primer Direction	Sequence (5' → 3')
<i>esxA</i>	Forward	TTAGGATCCGGGATGACAGAGCAGCAGTGG
	Reverse	GGCAAGCTTCCGCTATGCGAACATCCCAGTG
<i>esxB</i>	Forward	GGGTGAATTCGGGAATGGCAGAGATGAAGACCGATG
	Reverse	GGGAAGCTTGGGTCAGAAGCCCATTTGCGAGG
<i>esxM</i>	Forward	GTTGCTGCAGAGGGATGGCCTCACGTTTTATGAC
	Reverse	GTGAAGCTTGTCTAGCTGCTCAGGATCTGC
<i>esxN</i>	Forward	GGGTGAATTCGGGTATGACGATTAATTACCAGTTCGGG
	Reverse	GAGAAGCTTGAATTAGGCCAGCTGGAGCCGAC
<i>phoP</i>	Forward	GGGGAAGCTTAGGGATGCGGAAAGGGGTTGAT
	Reverse	TTTGTTAACGGGTCATCGAGGCTCCCGCAGTA
<i>phoR</i>	Forward	GTTGAAGCTTGGGATGGCCAGACACCTTCGAG
	Reverse	AAAGTTAACGAGTCAGGGCGGCCCTGGCAC

**Figure 6: PCR Primer Sequences.** Sequences of primers used in PCR for each gene.

Insert	Empty Plasmid	Restriction Enzymes
<i>esxA</i>	pUAB300	BamHI and HindIII
<i>esxB</i>	pUAB400	EcoRI and HindIII
<i>esxM</i>	pUAB300	PstI and HindIII
<i>esxN</i>	pUAB400	EcoRI and HindIII
<i>phoP</i>	pUAB300	HindIII and HpaI
<i>phoR</i>	pUAB400	HindIII and HpaI

**Figure 7: Restriction Enzymes.** Restriction enzymes used for each insert and plasmid.

After the plasmid vectors were formed, they were transformed into *E. coli*, which were grown on selectivity plates to ensure successful growth of only *E. coli* colonies with the desired plasmids. After an overnight growth of the selected colonies from the plates in liquid medium, plasmid purification was performed to isolate a large quantity of the desired plasmids. Then, the

success of the plasmid constructs was confirmed through gel electrophoresis and sequencing. Finally, electroporation of *Msm* cells was induced in order to create recombinant cells necessary for the M-PFC assay. The transformed bacteria were then grown on Hygromycin and Kanamycin plates to select for *Msm* recombinant cells that contain our plasmids of interest (New England BioLab Inc., 2014).

### **Drug Screening to Determine Interference of Protein Interactions**

After desired *Msm* recombinant cells were isolated, the M-PFC assay was performed with our drug panel. The M-PFC assay measures protein-protein interactions by correlating it to cell growth in the presence of an antibiotic. The drug screen used triplicate wells of a 96-well plate consisting of the *Msm* recombinant cells and their fusion proteins at the minimum effective concentration, the antibiotic, TRIM, growth media, and the solvent, DMSO. Drugs that blocked protein-protein interactions prevented the cells from growing in TRIM, whereas drugs that did not interfere in the interaction resulted in cell death (Mai et al., 2011). Cell growth was noted as a negative result and cell death was noted as a positive result. Cells which survived and digested the Alamar Blue into a product that exhibited a pink color measured at 562 nm. Wells of interest were those that displayed a 75% reduction in absorbance relative to the solvent control.

### **Origin of the Compound Library Source**

NIH's Clinical Collection provided the drug library used in this experiment. This library includes plated arrays of 725 small molecules with known health benefits. Many of these drugs were originally designed for other diseases, but may have untapped potential in disrupting mycobacterial biological pathways. As these drugs have already passed clinical testing, they can be implemented more easily than new compounds. Ten plates of drugs are provided with the drug panel. The complete list of these compounds and their structures in each plate can be found

on the NIH Clinical Collection's website. 10  $\mu$ L of each drug were provided at 10 mM. The drug compounds were diluted to 200  $\mu$ M concentration in water in new 96-well plates.

### **Growth Assay**

Because optimal concentrations for *Msm* cells transformed with EsxA and EsxB (EsxAB), and EsxM and EsxN (EsxMN) are not established, an assay to assess growth was performed to identify these concentrations. The OD conversion at 600 nm for cell concentration is 1 OD =  $3 \times 10^8$  cells/mL. The positive control was created through genetic recombination of pUAB100 and 200 plasmids with a gene encoding for a eukaryotic transcriptional activator protein, GCN4 (Hope & Struhl, 1987). This was produced in *Msm* and replicated for our positive control line. Ultimately, GCN4 promotes high protein-protein interaction and confers antibiotic resistance. Conversely, our negative control consisted of pUAB300 and 400 plasmids without additional gene inserts, which do not display cellular growth in the presence of TRIM due to the absence of interacting protein pairs. These controls, alongside wild type *Msm* cells, were prepared at  $1.00 \times 10^6$  cells/mL and  $1.00 \times 10^5$  cells/mL, and EsxAB and EsxMN cell lines were prepared at concentrations of  $1.00 \times 10^7$ ,  $5.00 \times 10^6$ ,  $1.00 \times 10^6$ ,  $5.00 \times 10^5$ ,  $1.00 \times 10^5$ ,  $5.00 \times 10^4$ ,  $1.00 \times 10^4$ , and  $5.00 \times 10^3$  cells/mL. A background negative control was prepared with 7H9 liquid broth. The background negative control, positive control, negative control, wild type, and the transformants were dispensed on the 96-well plate as shown in **Figure 9**. The appropriate sample was added to each well, with each well having a final 1X TRIM content of 50  $\mu$ g/mL. The plate was wrapped in foil and incubated for 24 hours before 10% by volume Alamar Blue was added to each well. The plate was again wrapped in foil and incubated for 6-8 hours. Afterwards, the plate was read with an Anthos 2010 microplate reader at 562 nm with a reference wavelength at 620 nm.

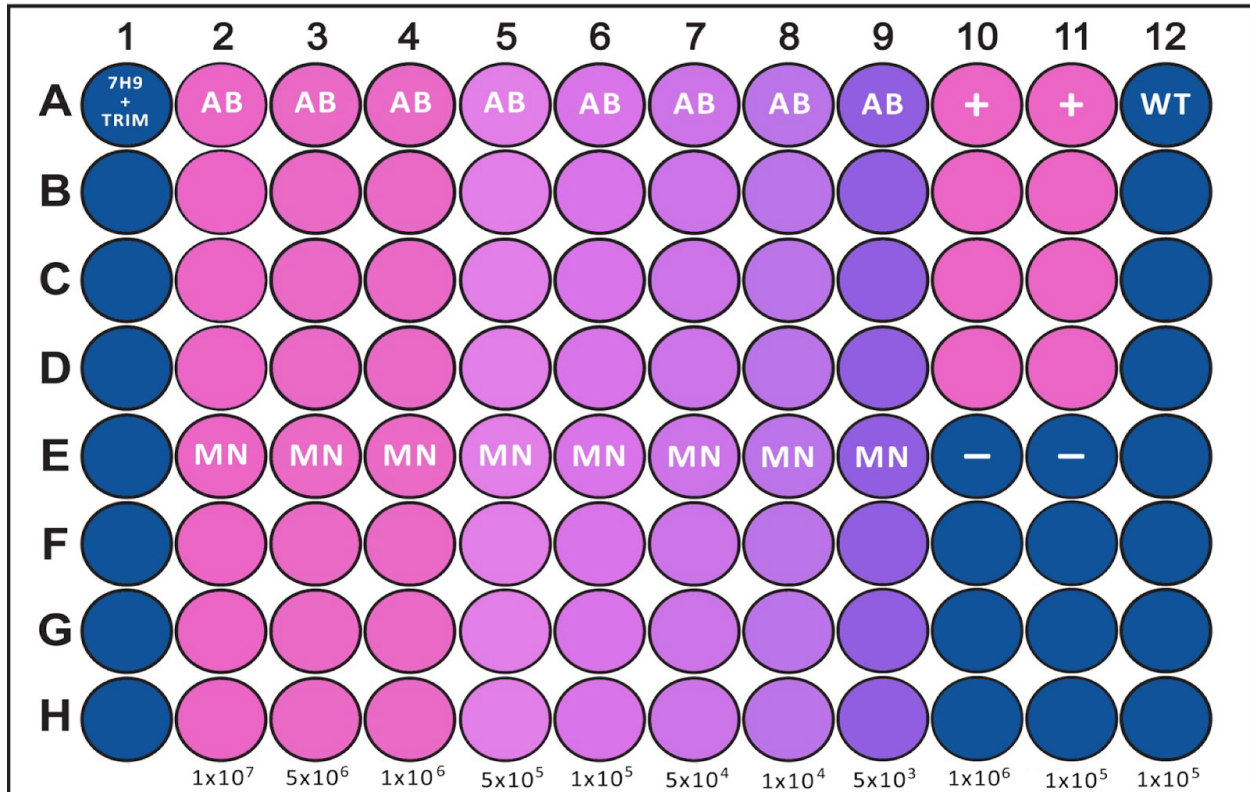


**Figure 8: Colorimetric Plate Assay.** Colorimetric plate assay demonstrating varying levels of cellular growth based on protein-protein interaction. Intensity of the pink color following TRIM treatment is proportional to the amount of TRIM resistant cells. *esxA*, *esxB*, *esxM*, and *esxN* are transformed into their respected empty plasmids and cells confer TRIM resistance. Positive control contains pUAB100 and pUAB200 interacting with a yeast protein. Negative control contains empty pUAB300 and pUAB400 plasmids.

### Drug Screening Layout

The OD were measured for overnight *Msm* cultures of EsxA-EsxB transformants, EsxM-EsxB transformants, EsxN transformants, positive control, and negative control. Each culture was diluted to the optimal cell concentration determined by the growth assay,  $5.55 \times 10^5$  cells/mL. **Figure 9** presents the layout of the wells for positive control, negative control, negative background control, vehicle control (transformed cells with DMSO, the solvent for the drugs), and the drug tests on the 96-well plate. The positive control, negative control, vehicle control, and negative background control wells contained 180  $\mu$ L of the appropriate  $5.55 \times 10^5$  cells/mL culture with 20  $\mu$ L of 5% DMSO to emulate the solvent conditions of the drugs. The drug test wells

contained 180  $\mu\text{L}$  of the transformed cells at  $5.55 \times 10^5$  cells/mL culture with 20  $\mu\text{L}$  of the diluted drugs in 5% DMSO. Final concentration of TRIM for all wells again was 50  $\mu\text{g/mL}$ . The plate was wrapped in foil and incubated for 24 hours before 20  $\mu\text{L}$  of Alamar Blue was added to all wells. The plate was again wrapped in foil and incubated from 6-8 hours. Afterwards, the plate was read with Anthos 2010 microplate reader.

## Chapter 3: Results

### Cloning Results

The PCR of the gene inserts (*esxA*, *B*, *M*, *N*) used the *Mtb* genomic DNA as a template. In order to create the plasmids to be used in the M-PFC assay, the M-PFC vectors and the inserts were ligated with their corresponding plasmids. The ligated plasmids were digested with restriction enzymes and placed on an agarose gel along with the empty M-PFC plasmids pUAB300 and 400 and the non-ligated inserts. The bands shown in **Figure 9** show that the inserts were successfully replicated due to having the correct size. *esxA* has a length of 312 bp. *esxB* has a length of 329 bp. *esxm* has a length of 323 bp. *esxN* has a length of 311 bp. Based on **Figure 9**, the insert bands on the gel were located below the 500 bp marker. Indicated in the top gel in the figure above are the successfully ligated *esxA* + pUAB300 and *esxB* + pUAB400 plasmids, which should be similar in length as the original M-PFC vectors. This indicates that the plasmids were successfully ligated. *esxM* + pUAB300 and *esxN* + pUAB400 were ligated with similar success. Unfortunately, the plasmids associated with *phoP* and *phoR* were not successfully ligated. The successfully constructed plasmids were then transformed into the *Msm* cell line for the M-PFC assay.



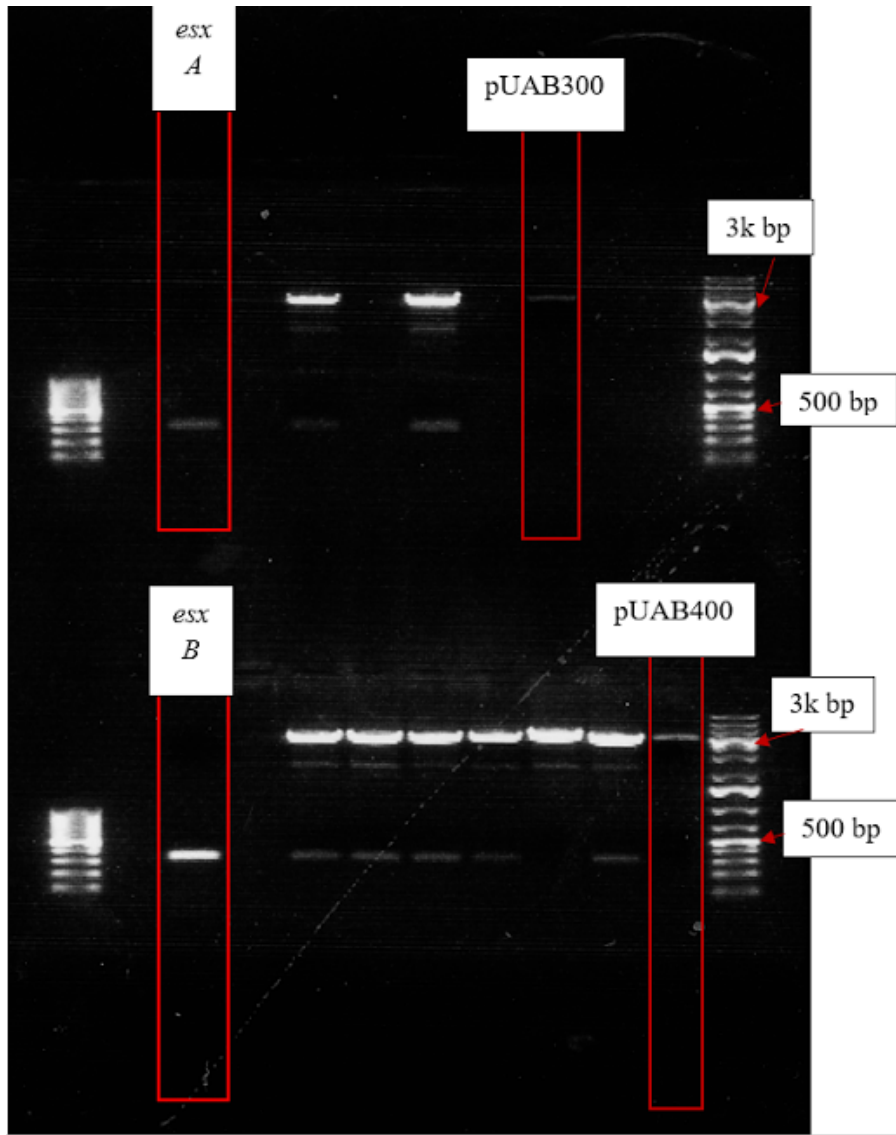


**Figure 9: Image of the Gel Containing the *esxA* and *esxB* Inserts.**

The bands located below 500 bp indicate that the *esxA* and *esxB* inserts were successfully replicated (both *esxA* and *esxB* are about 300 bp.) The bands of the ligated plasmid *esxA* + pUAB300 are located to the right of the *esxA* band, and the bands of the ligated plasmid *esxB* + pUAB400 are located to the right of the *esxB* band.

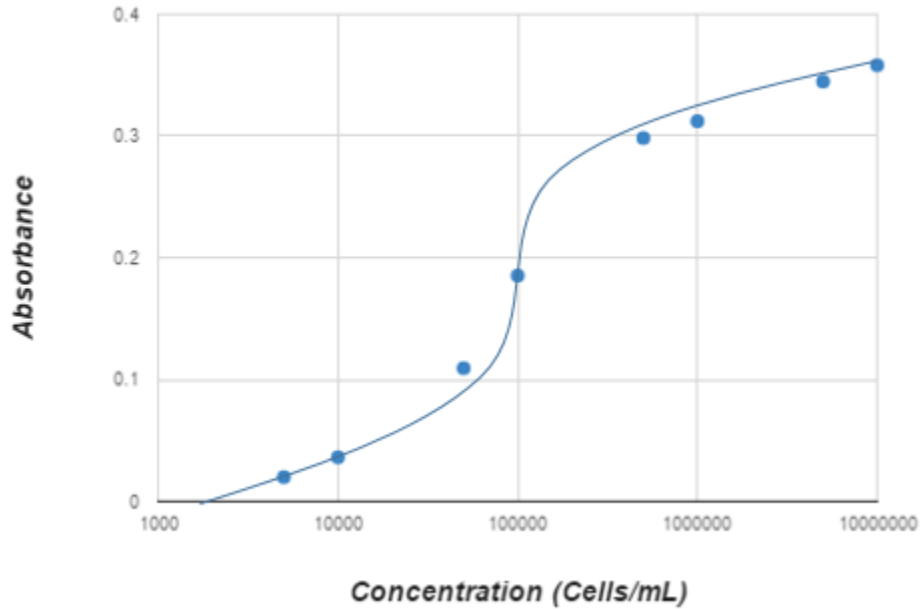


**Figure 10: Growth assay for EsxAB *Msm* transformants.** Cells were grown for 24 hours before Alamar Blue was added, and concentration was assessed using spectrophotometer at 562 nm with reference wavelength of 620 nm after 6 hours. From the plot, concentration of  $5 \times 10^5$  cells/mL will be used for screen.

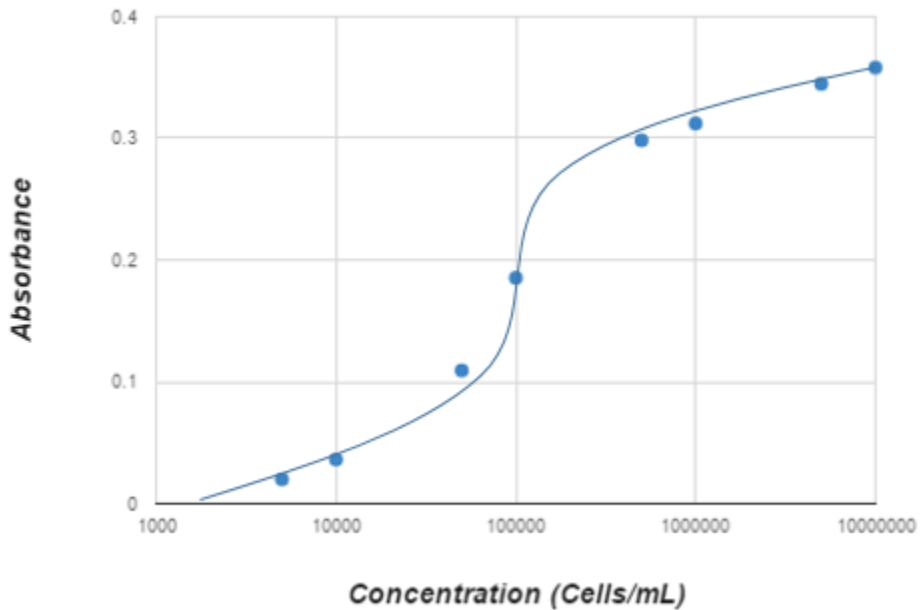


**Figure 11: Growth assay for EsxMN *Msm* transformants.** Cells were grown for 24 hours before Alamar Blue was added, and concentration was assessed using spectrophotometer at 562 nm with reference wavelength of 620 nm after 6 hours. From the plot, concentration of  $5 \times 10^5$  cells/mL will be used for screen.

Growth assay data represented graphically with absorbance plotted against the logarithmic scale of the cell concentration. The optimal cell concentration was determined to be the point at the end of the exponential point of the graph where there is the largest change in absorbance with a relatively small change in concentration. Cells were allowed to grow for 24 hours before Alamar Blue dye was added. Cells grew for an additional 6 hours before reading. For both cell lines in *Msm*, growth assay data appeared sigmoidal in shape, and the cell concentration that approached the top of the linear portion of the sigmoidal curve was  $5 \times 10^5$  cells/mL. Repeated trials of the growth plate corroborated the results shown in the **Figures 11 and 12**. Using this concentration will show the largest change in absorbance when inhibition occurs during screen.

#### M-PFC Assay Drug Screening Results

Cell Line of Unique Hit	Name of Compound	Percent Growth Inhibition	Compound Classification
AB	2-Chloroadenosine	81%	Adenosine receptor agonist
AB	Meclizine HCl	86%	Histamine H1 antagonist
MN	Carmofur	76%	Antineoplastic
MN	Cefdinir	90%	$\beta$ -lactam antibiotic, Cephalosporin
MN	5-Fluorouracil	82%	Antineoplastic
MN	Mefloquine HCl	87%	Antimalarial quinoline

MN	Ampicillin	95%	$\beta$ -lactam antibiotic
----	------------	-----	----------------------------

**Figure 12: Table of All Unique Positive Results for Both the EsxAB and EsxMN Cell Lines.** The cell line corresponding to the unique hit, the compound name and compound classification is listed in each row. Drugs which tested positive for each cell line were considered to have native cytotoxic activity and were not considered unique positive results.

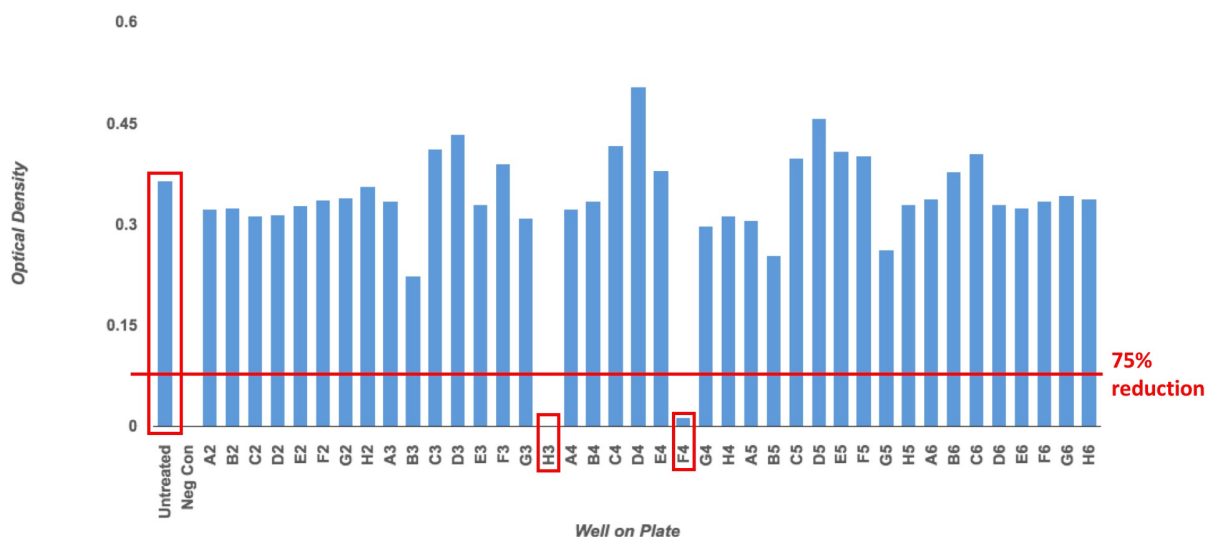


**Figure 13: Absorbance Data for Plate NCP004205 Tested Against the EsxMN Cell Line.** This figure displays the results of the screen of the EsxMN cell line with compound plate NCP004205. Graph showing absorbance values of individual wells. The red line across the bar graph represents threshold for positive hits at absorbance of 0.089. Positive hits were taken as at least a 75% reduction in absorbance of the untreated cells, whose absorbance value is shown by the leftmost bar.

While we chose to use a simple absorbance readout at 562 nm with a 620 nm reference, it should be noted that we used the same 75% reduction cutoff as previous work. In our case, we compared absorbance reduction as opposed to fluorescence reduction. Our NCP004205 plate in **Figure 13** depicts a typical analysis of absorbance data. For simplicity, the other 19 graphs of our absorbance data were omitted and **Figure 12** has been included as a model. While the tuberculosis necrotizing toxin (TNT)-immunity factor for TNT (IFT) pair cell line used by another group member previously produced 44 positive results with the same drug panel, our EsxAB cell line had 48 positive results and our EsxMN had 51. Of these, 46 were found to

overlap and deemed as non-specific growth inhibitors of *Msm*. Our nonspecific 46 results showed good agreement with the 44 found by the TNT-IFT cell line. The two unique hits for EsxAB and the five for EsxMN are shown in **Figure 12** along with their percent growth inhibition values in their individual assays. We chose to focus on the unique hits for the remainder of our discussion. All of the positive results are listed in Appendix B.

## Chapter 4: Discussion

The positive results shown in **Figure 12** have yet to be evaluated to determine reproducibility as the screen was designed with the idea of being high-throughput and, as a result, data was only obtained in a single replicate for each compound for a screen. All of the compounds listed will be screened against both the EsxAB and EsxMN cell lines again in addition to being tested against our pUAB100 and 200 positive control cell line. Only if the drug tests positive for growth inhibition against one of the cell lines without being positive against the other two will it be considered a true positive. We will discuss all of the drugs in **Figure 12** for their possibility as a unique inhibitor of the EsxAB or EsxMN interaction.

### Cefdinir and Ampicillin

Cefdinir and Ampicillin both belong to the penicillin family of antibiotics, which contain the four-membered  $\beta$ -lactam ring and inhibit the cross-linking of peptidoglycan chains in the bacterial cell wall, causing lysis of the bacterium. Cefdinir falls under the sub-classification of  $\beta$ -lactam antibiotics known as cephalosporins for originating from the fungus *Acremonium*. Cefdinir and Ampicillin have been tested against a variety of mycobacterial species to assess their viabilities for treating *Mtb* as well as *M. avium*. infections. Each of the drugs exhibited native cytotoxic activity against mycobacteria. Again, we have not had the opportunity to test these antibiotics against each of the cells lines, but we expect that upon testing again, we should see nonspecific cytotoxic activity. Also informing our hypothesis is that drugs such as penicillin and amoxicillin were included in this drug library but did not show specific killing activity for either of the cell lines (Gold et al., 2016; Ramon-Garcia et al., 2016).

### **Carmofur and 5-Fluorouracil**

Carmofur and 5-fluorouracil are both modified nucleotides, which have been used for decades because of their antineoplastic activity. Both drugs show micromolar activity against *Mtb*. The best supported mechanism of action of these compounds in mycobacteria is their ability to inhibit the cell-wall biosynthesis. As both carmofur and 5-fluorouracil have shown to have native *Mtb* killing activity, we believe that both of these results will show as false positives when rescreened against both the positive control and EsxAB cell lines (Singh et al., 2015; Takenaka et al., 1995).

### **Mefloquine**

Mefloquine is typically used in the treatment of chloroquine-sensitive *P. falciparum* malaria. As a derivative of the prototypical anti-malarial chloroquine, it inhibits the parasite's ability to digest hemoglobin and crystalize heme. Both of these steps are critical for the ability of malaria to escape the erythrocyte and continue infecting red blood cells. Mefloquine has shown inherent inhibiting activity against *Mtb* in previous studies. While it is possible that the intracellular target of the drug is the EsxMN interaction, studies have shown that mefloquine is toxic to mycobacteria when in an *in vivo* mouse model and against free *Mtb in vitro*. Mefloquine has shown the remarkable ability to penetrate the host macrophage and phagosome in order to reach and kill the bacteria but the mechanism of action is most likely not related to inhibition of EsxMN. In addition, the recent study from our lab group specifically identified mefloquine as cytotoxic against *Msm*. We expect further testing this result will support our current hypothesis (Bermudez et al., 1999; Rodrigues-Junior et al., 2016).

## **2-Chloroadenosine**

2-chloroadenosine is commonly used as an adenosine-receptor agonist, which gives this compound large effects on both the nervous and immune systems. Previous work has evaluated 2-chloroadenosine for its potential as an antimycobacterial agent. The study identified that the drug exerted growth inhibiting activity against both wild-type *Mtb* and BCG in liquid culture but not against *Msm*. Our positive result for our EsxAB could mean that we observed inhibition of our protein-protein interaction but, as previously explained, the EsxA-EsxB interaction is not vital for the viability of the bacterium in liquid culture. The apparent cytotoxicity exclusively against our cells is still of note as prior research has shown that we should not expect the observed activity. However, if 2-chloroadenosine does inhibit the EsxA-EsxB interaction leading to the death of our model cell line, its mechanism of action against different strains of *Mtb* must include another cellular target important to the vitality of the bacterium in free solution. While this result awaits duplication, we believe that part of 2-chloroadenosine's action against *Mtb* may be related to inhibiting EsxAB dimer formation, although this activity is not naturally cytotoxic to the mycobacterium (Altaf et al., 2010).

## **Meclizine**

Meclizine is typically used for the treatment of nausea, vertigo, and motion sickness in pregnant women and patients suffering from diseases that affect the vestibular apparatus. The drug functions as a histamine H1 antagonist and has not been evaluated for antimycobacterial activity to our knowledge. Our group lacks the software to predict why meclizine would inhibit the formation of the EsxAB dimer. EsxA-EsxB bind with an imidazole molecule in between them but meclizine does not bear resemblance to imidazole. While we are unable to confidently conjecture how meclizine may interfere with the EsxAB dimer, our preliminary results suggest



that this may be a novel agent for interfering with a vital virulence pathway of *Mtb* (Yerushalmy & Milkovich, 1965; Simons, 1989).

### **Proof of Concept**

Previous work by the Briken lab has established a screen similar to ours to test the same NIH Clinical Collection of compounds. However, in the past work, the readout was taken by utilizing the fluorescent nature of Alamar Blue while our study used a pure absorbance based readout. **Figures 11 and 12** illustrate the ability of our dye to monitor cell growth by quantifying absorbance of light at 562 nm. In addition, previous work by Mai *et. al.* showed that a high-throughput screening method could be established with the aid of robots. Our work was accomplished without the assistance of automation. Therefore, we have established a robust, high-throughput screening method to test potential inhibitors of the EsxAB and EsxMN interactions without automation and only utilizing a simple absorbance based readout. The present screen lacked access to known inhibitors of the protein-protein interactions which would be needed to confirm that the efficacy of this method. In addition to the potential inhibitors we have identified in our work, our screen possess the potential to be used as a high-throughput method for finding specific inhibitors of virulence pathways of *Mycobacterium tuberculosis* (Mai et al., 2011; Singh et al., 2006).

### **Limitations**

The greatest limitation of our work was the inability to perform all trials in at least duplicate, which came about as a combination of factors. Lab work space was only conducive to performing trials as single replicates in a time-efficient manner. In addition, we had a limited amount of each compound provided by the NIH. However, our results are easy to verify by

performing the screen again or, in our case, testing specific, unique positive results to see if they do inhibit our protein-protein interaction.

### **Future Implications**

We believe that our studies have created two very important implications for future work. We have generated a high-throughput drug screen to test small molecules to see if they inhibit protein-protein interactions in *Mtb* without the use of automation or fluorescence. In addition, we have identified two molecules, meclizine and 2-chloroadenosine, that we believe may inhibit formation of the EsxAB dimer in *Mtb*. We hope to retest the results from our screen to identify if our hits were, in fact, inhibitors of the proteins we were targeting.

## Chapter 5: Conclusion

The first aim was to establish a high-throughput drug screen. Our screen, along with the other similar work from our lab have shown that the M-PFC system can be very robust in testing small molecules for their ability to inhibit protein-protein interactions of *Mtb*. In addition, we were able to investigate specific molecules which had positive results from our screen for their potential to inhibit the formation of the EsxAB and EsxMN dimers. The experiments we performed identified 46 molecules in the NIH Clinical Collection that possessed nonspecific growth inhibition, in that they affected both the EsxAB and EsxMN cell lines. Seven molecules were identified for their ability to selectively inhibit one of the two cell lines. We need to test these molecules again to confirm their specific activity but we believe that at least two of the seven show promise in selectively inhibiting a virulence pathway of *Mtb*.

## Appendix A: Protocols

### 7H11 Plates

This protocol makes roughly 40 plates.

1. Pour 21 g of 7H11 mix into 900 mL of dH<sub>2</sub>O.
2. Autoclave it on liquid cycle (takes ~ 1-2 hours).
3. Take out the ADC from the the cell culture refrigerator and leave it on the bench so that it reaches room temperature.
4. Wait for it to cool until cool enough to touch (leave it in the 55°C water block).  
**-- make sure the following steps are done under the hood --**
5. Add 5 mL of sterile 100% glycerol (10 mL if we use 50% glycerol).
6. Add antibiotics (1 mL for 1 L for Kanamycin & Hygromycin).
7. Add 100 mL of ADC (100mL for 1 L).
8. Label the plates.
9. Use the serological pipet to transfer 25 mL of the 7H11 media into the plate.
10. Let it cool.
11. When the plates solidify, put the plates in the 4°C fridge.

### DNA Gel Electrophoresis with TAE, 1% gel

1. Load 5 µg of DNA ladder (GeneRuler 100 bp DNA Ladder)
2. 10 µL of 6x DNA loading dye in 50 µL of PCR product
3. Load all 60 µL of dye + PCR product into gel well. Separate each by one well so it is easier to cut/won't mix together
4. Set FB300 power unit to 120 V and run gel, bump up to 120 V to make it go faster (keep eye on blue dye moving).
5. When placing gel into the tray, take off the tape you used to secure the gel in place.
6. Visualize bands in dark room using tray. Clean first, wear long sleeve!
7. Cut band between 1st and 2nd below fat band in middle used for orientation using razor blade.
8. Put gel pieces with desired DNA in Eppendorf tubes and label them.
9. Place in -20°C freezer in box.
10. Dispose of gel waste in EtBr waste, dispose razor blades in sharps waste.

### Making Medium

- Liquid LB Medium
  - a. 25 g liquid LB powder
  - b. 1 L H<sub>2</sub>O
  - c. Autoclave on fluid cycle
- 20% TWEEN-80
  - . 4 mL 100% TWEEN-80
  - a. 16 mL H<sub>2</sub>O
  - b. TWEEN-80 MUST be kept sterile
  - c. Use autoclave water to save time from filtering
- Stock 40% Dextrose
  - . 200 g dextrose

- a. 500 mL H<sub>2</sub>O
- b. Get stir bar ahead of time
- c. Stir immediately after mixing dextrose and H<sub>2</sub>O
- d. Dissolve dextrose in <500 mL and fill up to 500 mL after

### **Autoclaving**

1. Each type of autoclaved agent has a different button (e.g. liquid for liquids)
2. Stand towards the hinges when opening door to avoid burns
3. Close tightly, but not so tightly so that it cannot be opened later
4. Never screw caps on all the way
5. Use autoclave tape
6. Keep things with autoclave tape in Biohazard Safety Cabinet
7. Steps in the autoclave room:
  - a. Close
  - b. Press yellow/orange button for Fluid Cycle
  - c. Press "on"
  - d. Be careful when opening the autoclave
  - e. Put the setting on 20 min cycle and cool down
  - f. Close the door tightly but not too tightly

### **Innoculated *Msm* cultures in growth medium (wild type + positive control)**

1. Use glass beads to help with stirring (3-5 beads)
  - a. using turbid solution, doing dilution of 1:10 so doubles every six hours
2. 5 mL growth medium and 550 µL culture (for living cultures use filter tips)
3. Pipette in vespine disinfectant and dispose in biohazard waste when done
4. Incubate cultures in *Msm* incubator for 18 hours (overnight); no *E. coli* in that incubator
5. Move to +4°C fridge

### **Transformation of Competent *E. coli* Cells**

1. Remove *E. coli* competent cells from the -80°C freezer and thaw on ice.
2. Into the cells into 50 µL of cells introduce 5 µL of DNA. Mix gently using the pipette tip.
3. 2nd tube: just plasmid, no insert.
4. Incubate on ice for 30 minutes.
5. Transfer tube to 42°C heating block for 1 min to heat shock the cells. Put water in wells to hold heat better.
6. Move the tube back on ice immediately for 2 mins.
7. At the end of 2 mins, add 1mL of LB medium to the cells. Incubate in shaker in 37°C for 1 hour.
  - a. During this time prewarm the LB agar plates (with appropriate antibiotic) in the 37°C incubator.
8. At the end of the 1-hour incubation, plate 50 µL of culture. Spin the remaining *E. coli* cells at 8000 rpm/1min. Discard the supernatant, leaving about 100 µL behind the tube. Resuspend the cells.
9. Plate the entire volume on a LB agar plate and incubate at 37°C overnight.

**Appendix B: All Positive Results for Both Cell Lines using the M-PFC System**

<b>Drug Name</b>	<b>Positive for EsxAB</b>	<b>Positive for EsxMN</b>
CLARITHROMYCIN	Yes	Yes
TOSUFLOXACIN TOSILATE	Yes	Yes
PAZUFLOXACIN	Yes	Yes
KITASAMYCIN	Yes	Yes
ENROFLOXACIN	Yes	Yes
ETOPOSIDE	Yes	Yes
IDARUBICIN HYDROCHLORIDE	Yes	Yes
CLOFAZIMINE	Yes	Yes
LEVOFLOXACIN	Yes	Yes
TEGASEROD MALEATE	Yes	Yes
RIFAPENTINE	Yes	Yes
TRIFLUOPERAZINE HCl	Yes	Yes
RIFABUTIN	Yes	Yes
LINEZOLID	Yes	Yes
RIFAXIMIN	Yes	Yes
DOXORUBICIN HYDROCHLORIDE	Yes	Yes
EPIRUBICIN HYDROCHLORIDE	Yes	Yes
RUFLOXACIN MONOHYDROCHLORIDE	Yes	Yes
PEFLOXACIN MESYLATE	Yes	Yes
MOXIFLOXACIN HYDROCHLORIDE	Yes	Yes
ETHAMOBUTOL	Yes	Yes
LINCOMYCIN HCl	Yes	Yes

OFLOXACIN	Yes	Yes
70458-96-7	Yes	Yes
RIFAPENTINE	Yes	Yes
DAUNORUBICIN HYDROCHLORIDE	Yes	Yes
MERCAPTOPURINE	Yes	Yes
MINOCYCLINE HYDROCHLORIDE	Yes	Yes
PYRIMETHAMINE	Yes	Yes
DOXYCYCLINE	Yes	Yes
BETAMETHASONE	Yes	Yes
OXYTETRACYCLINE HYDROCHLORIDE	Yes	Yes
DEMECLOCYLINE	Yes	Yes
SULFISOXAZOLE	Yes	Yes
CEFOXITIN	Yes	Yes
TETRACYCLINE	Yes	Yes
SULFAMETHOXAZOLE	Yes	Yes
CHLORAMPHENICOL	Yes	Yes
SULFACETAMIDE	Yes	Yes
AZITHROMYCIN	Yes	Yes
MITOXANTRONE	Yes	Yes
DAPSONE	Yes	Yes
RIFAMPICIN	Yes	Yes
RIFABUTIN	Yes	Yes
SPECTINOMYCIN DIHYDROCHLORIDE PENTAHYDRATE	Yes	Yes
ERYPED	Yes	Yes
2-CHLOROADENOSINE	Yes	No

MECLIZINE HYDROCHLORIDE	Yes	No
MEFLOQUINE HYDROCHLORIDE	No	Yes
AMPICILLIN SODIUM	No	Yes
5-FLUOROURACIL	No	Yes
CARMOFUR	No	Yes
CEFDINIR	No	Yes



## References

- Abate, G., Aseffa, A., Selassie, A., Goshu, S., Fekade, B., WoldeMeskal, D., & Miorner, H. (2004). Direct colorimetric assay for rapid detection of rifampin-resistant *Mycobacterium tuberculosis*. *J Clin Microbiol*, *42*(2), 871-873.
- Abate, G., Mshana, R. N., & Miorner, H. (1998). Evaluation of a colorimetric assay based on 3-(4,5-dimethylthiazol-2-yl)-2,5-diphenyl tetrazolium bromide (MTT) for rapid detection of rifampicin resistance in *Mycobacterium tuberculosis*. *Int J Tuberc Lung Dis*, *2*(12), 1011-1016.
- Abdallah, A. M., Bestebroer, J., Savage, N. D., de Punder, K., van Zon, M., Wilson, L., Peters, P. J. (2011). Mycobacterial secretion systems ESX-1 and ESX-5 play distinct roles in host cell death and inflammasome activation. *J Immunol*, *187*(9), 4744-4753. doi:10.4049/jimmunol.1101457
- Abdallah, A. M., Gey van Pittius, N. C., Champion, P. A., Cox, J., Luirink, J., Vandenbroucke-Grauls, C. M., Bitter, W. (2007). Type VII secretion--mycobacteria show the way. *Nat Rev Microbiol*, *5*(11), 883-891. doi:10.1038/nrmicro1773
- Abdallah, A. M., Savage, N. D., van Zon, M., Wilson, L., Vandenbroucke-Grauls, C. M., van der Wel, N. N., Bitter, W. (2008). The ESX-5 secretion system of *Mycobacterium marinum* modulates the macrophage response. *J Immunol*, *181*(10), 7166-7175.
- Alderson, M. R., Bement, T., Day, C. H., Zhu, L., Molesh, D., Skeiky, Y. A., ... & Dillon, D. C. (2000). Expression cloning of an immunodominant family of *Mycobacterium tuberculosis* antigens using human CD4+ T cells. *Journal of Experimental Medicine*, *191*(3), 551-560.
- Altaf, M., Miller, C. H., Bellows, D. S., & O'Toole, R. (2010). Evaluation of the *Mycobacterium smegmatis* and BCG models for the discovery of *Mycobacterium tuberculosis* inhibitors. *Tuberculosis (Edinb)*, *90*(6), 333-337. doi:10.1016/j.tube.2010.09.002

- Ates, L. S., & Brosch, R. (2017). Discovery of the type VII ESX-1 secretion needle? *Mol Microbiol*, *103*(1), 7-12. doi:10.1111/mmi.13579
- Ates, L. S., Ummels, R., Commandeur, S., van de Weerd, R., Sparrius, M., Weerdenburg, E., Houben, E. N. (2015). Essential Role of the ESX-5 Secretion System in Outer Membrane Permeability of Pathogenic Mycobacteria. *PLoS Genet*, *11*(5), e1005190. doi:10.1371/journal.pgen.1005190
- Basic TB Facts. (2016, March 20). Retrieved April 30, 2017, from <https://www.cdc.gov/tb/topic/basics/default.htm>
- Bean, A. G., Roach, D. R., Briscoe, H., France, M. P., Korner, H., Sedgwick, J. D., & Britton, W. J. (1999). Structural deficiencies in granuloma formation in TNF gene-targeted mice underlie the heightened susceptibility to aerosol Mycobacterium tuberculosis infection, which is not compensated for by lymphotoxin. *J Immunol*, *162*(6), 3504-3511.
- Bedard, K., & Krause, K. H. (2007). The NOX family of ROS-generating NADPH oxidases: physiology and pathophysiology. *Physiol Rev*, *87*(1), 245-313. doi:10.1152/physrev.00044.2005
- Behar, S. M., Martin, C. J., Booty, M. G., Nishimura, T., Zhao, X., Gan, H. X., Remold, H. G. (2011). Apoptosis is an innate defense function of macrophages against Mycobacterium tuberculosis. *Mucosal Immunol*, *4*(3), 279-287. doi:10.1038/mi.2011.3
- Bermudez, L. E., Kolonoski, P., Wu, M., Aralar, P. A., Inderlied, C. B., & Young, L. S. (1999). Mefloquine Is Active In Vitro and In Vivo against Mycobacterium avium Complex. *Antimicrobial agents and chemotherapy*, *43*(8), 1870-1874.
- Bohsali, A., Abdalla, H., Velmurugan, K., & Briken, V. (2010). The non-pathogenic mycobacteria M. smegmatis and M. fortuitum induce rapid host cell apoptosis via a caspase-3 and TNF dependent pathway. *BMC microbiology*, *10*(1), 237.

- Bottai, D., Di Luca, M., Majlessi, L., Frigui, W., Simeone, R., Sayes, F., Esin, S. (2012). Disruption of the ESX-5 system of *Mycobacterium tuberculosis* causes loss of PPE protein secretion, reduction of cell wall integrity and strong attenuation. *Mol Microbiol*, 83(6), 1195-1209.  
doi:10.1111/j.1365-2958.2012.08001.x
- Brodin, P., de Jonge, M. I., Majlessi, L., Leclerc, C., Nilges, M., Cole, S. T., & Brosch, R. (2005). Functional analysis of early secreted antigenic target-6, the dominant T-cell antigen of *Mycobacterium tuberculosis*, reveals key residues involved in secretion, complex formation, virulence, and immunogenicity. *J Biol Chem*, 280(40), 33953-33959.  
doi:10.1074/jbc.M503515200
- Callahan, B., Nguyen, K., Collins, A., Valdes, K., Caplow, M., Crossman, D. K., Derbyshire, K. M. (2010). Conservation of structure and protein-protein interactions mediated by the secreted mycobacterial proteins EsxA, EsxB, and EspA. *J Bacteriol*, 192(1), 326-335.  
doi:10.1128/jb.01032-09
- Chan, E. D., Winston, B. W., Uh, S. T., Wynes, M. W., Rose, D. M., & Riches, D. W. (1999). Evaluation of the role of mitogen-activated protein kinases in the expression of inducible nitric oxide synthase by IFN-gamma and TNF-alpha in mouse macrophages. *J Immunol*, 162(1), 415-422.
- Clark, K. L., Larsen, P. B., Wang, X., & Chang, C. (1998). Association of the Arabidopsis CTR1 Raf-like kinase with the ETR1 and ERS ethylene receptors. *Proc Natl Acad Sci U S A*, 95(9), 5401-5406.
- Daleke, M. H., Cascioferro, A., de Punder, K., Ummels, R., Abdallah, A. M., van der Wel, N., Bitter, W. (2011). Conserved Pro-Glu (PE) and Pro-Pro-Glu (PPE) protein domains target LipY lipases of

- pathogenic mycobacteria to the cell surface via the ESX-5 pathway. *J Biol Chem*, 286(21), 19024-19034. doi:10.1074/jbc.M110.204966
- Daleke, M. H., Ummels, R., Bawono, P., Heringa, J., Vandenbroucke-Grauls, C. M., Luirink, J., & Bitter, W. (2012). General secretion signal for the mycobacterial type VII secretion pathway. *Proc Natl Acad Sci U S A*, 109(28), 11342-11347. doi:10.1073/pnas.1119453109
- Di Luca, M., Bottai, D., Batoni, G., Orgeur, M., Aulicino, A., Counoupas, C., Esin, S. (2012). The ESX-5 associated eccB-EccC locus is essential for Mycobacterium tuberculosis viability. *PLoS One*, 7(12), e52059. doi:10.1371/journal.pone.0052059
- Dietrich, J., Doherty, M. T. (2009). Interaction of mycobacterium tuberculosis with the host: Consequences for vaccine development. *Apmis*, 117(5-6), 440-457.
- Dziedzic, R., Kiran, M., Plocinski, P., Ziolkiewicz, M., Brzostek, A., Moomey, M., Rajagopalan, M. (2010). Mycobacterium tuberculosis ClpX interacts with FtsZ and interferes with FtsZ assembly. *PLoS One*, 5(7), e11058. doi:10.1371/journal.pone.0011058
- Elliott, S. R., & Tischler, A. D. (2016). Phosphate starvation: a novel signal that triggers ESX-5 secretion in Mycobacterium tuberculosis. *Mol Microbiol*, 100(3), 510-526. doi:10.1111/mmi.13332
- Flynn, J. L., & Chan, J. (2001). Immunology of tuberculosis. *Annu Rev Immunol*, 19, 93-129. doi:10.1146/annurev.immunol.19.1.93
- Gey van Pittius, N. C., Sampson, S. L., Lee, H., Kim, Y., van Helden, P. D., & Warren, R. M. (2006). Evolution and expansion of the Mycobacterium tuberculosis PE and PPE multigene families and their association with the duplication of the ESAT-6 (esx) gene cluster regions. *BMC Evol Biol*, 6, 95. doi:10.1186/1471-2148-6-95
- Global tuberculosis report 2013*. (2013). In: World Health Organization.

- Gold, B., Smith, R., Nguyen, Q., Roberts, J., Ling, Y., Lopez Quezada, L., Aube, J. (2016). Novel Cephalosporins Selectively Active on Nonreplicating Mycobacterium tuberculosis. *J Med Chem*, 59(13), 6027-6044. doi:10.1021/acs.jmedchem.5b01833
- Guinn, K. M., Hickey, M. J., Mathur, S. K., Zakel, K. L., Grotzke, J. E., Lewinsohn, D. M., Sherman, D. R. (2004). Individual RD1-region genes are required for export of ESAT-6/CFP-10 and for virulence of Mycobacterium tuberculosis. *Mol Microbiol*, 51(2), 359-370. doi:10.1046/j.1365-2958.2003.03844.x
- Hope, I. A., & Struhl, K. (1987). GCN4, a eukaryotic transcriptional activator protein, binds as a dimer to target DNA. *Embo j*, 6(9), 2781-2784.
- Houben, D., Demangel, C., van Ingen, J., Perez, J., Baldeon, L., Abdallah, A. M., Peters, P. J. (2012a). ESX-1-mediated translocation to the cytosol controls virulence of mycobacteria. *Cell Microbiol*, 14(8), 1287-1298. doi:10.1111/j.1462-5822.2012.01799.x
- Houben, E. N., Bestebroer, J., Ummels, R., Wilson, L., Piersma, S. R., Jimenez, C. R., Bitter, W. (2012b). Composition of the type VII secretion system membrane complex. *Mol Microbiol*, 86(2), 472-484. doi:10.1111/j.1365-2958.2012.08206.x
- Houben, E. N., Korotkov, K. V., & Bitter, W. (2014). Take five - Type VII secretion systems of Mycobacteria. *Biochim Biophys Acta*, 1843(8), 1707-1716. doi:10.1016/j.bbamcr.2013.11.003
- Hutchings, M. I., Hoskisson, P. A., Chandra, G., & Buttner, M. J. (2004). Sensing and responding to diverse extracellular signals? Analysis of the sensor kinases and response regulators of *Streptomyces coelicolor* A3(2). *Microbiology*, 150(9), 2795-2806. doi:doi:10.1099/mic.0.27181-0
- Kaufmann, S. H. (2013). Tuberculosis vaccines: time to think about the next generation. *Semin Immunol*, 25(2), 172-181. doi:10.1016/j.smim.2013.04.006

- Keshavjee, S., & Farmer, P. E. (2012). Tuberculosis, drug resistance, and the history of modern medicine. *N Engl J Med*, *367*(10), 931-936. doi:10.1056/NEJMra1205429
- Kumar, V., Abbas, A. K., & Aster, J. C. (2012). *Robbins basic pathology*. In (Vol. 9th edition, pp. 493-499).
- Lou, Y., Rybniker, J., Sala, C., & Cole, S. T. (2017). EspC forms a filamentous structure in the cell envelope of *Mycobacterium tuberculosis* and impacts ESX-1 secretion. *Mol Microbiol*, *103*(1), 26-38. doi:10.1111/mmi.13575
- Mai, D., Jones, J., Rodgers, J. W., Hartman, J. L. t., Kutsch, O., & Steyn, A. J. (2011). A screen to identify small molecule inhibitors of protein-protein interactions in mycobacteria. *Assay Drug Dev Technol*, *9*(3), 299-310. doi:10.1089/adt.2010.0326
- Martin, C., Williams, A., Hernandez-Pando, R., Cardona, P. J., Gormley, E., Bordat, Y., Gicquel, B. (2006). The live *Mycobacterium tuberculosis* phoP mutant strain is more attenuated than BCG and confers protective immunity against tuberculosis in mice and guinea pigs. *Vaccine*, *24*(17), 3408-3419. doi:http://dx.doi.org/10.1016/j.vaccine.2006.03.017
- Martín, J.-F., & Liras, P. (2010). Engineering of regulatory cascades and networks controlling antibiotic biosynthesis in *Streptomyces*. *Current Opinion in Microbiology*, *13*(3), 263-273. doi:http://dx.doi.org/10.1016/j.mib.2010.02.008
- Michod, R. E., Bernstein, H., & Nedelcu, A. M. (2008). Adaptive value of sex in microbial pathogens. *Infect Genet Evol*, *8*(3), 267-285. doi:10.1016/j.meegid.2008.01.002
- Miller, J. L., Velmurugan, K., Cowan, M. J., & Briken, V. (2010). The type I NADH dehydrogenase of *Mycobacterium tuberculosis* counters phagosomal NOX2 activity to inhibit TNF-alpha-mediated host cell apoptosis. *PLoS Pathog*, *6*(4), e1000864. doi:10.1371/journal.ppat.1000864
- Molecular Cloning Technical Guide. (2014). In: New England BioLab Inc.

- Müller, I., Cobbold, S. P., Waldmann, H., & Kaufmann, S. H. (1987). Impaired resistance to Mycobacterium tuberculosis infection after selective in vivo depletion of L3T4+ and Lyt-2+ T cells. *Infect Immun*, 55(9), 2037-2041.
- Penuelas-Urquides, K., Villarreal-Trevino, L., Silva-Ramirez, B., Rivadeneyra-Espinoza, L., Said-Fernandez, S., & de Leon, M. B. (2013). Measuring of Mycobacterium tuberculosis growth. A correlation of the optical measurements with colony forming units. *Braz J Microbiol*, 44(1), 287-289. doi:10.1590/s1517-83822013000100042
- Pym, A. S., Brodin, P., Brosch, R., Huerre, M., & Cole, S. T. (2002). Loss of RD1 contributed to the attenuation of the live tuberculosis vaccines Mycobacterium bovis BCG and Mycobacterium microti. *Mol Microbiol*, 46(3), 709-717.
- Ryndak, M., Wang, S., Smith, I. (2008). PhoP, a key player in mycobacterium tuberculosis virulence. *Trends in Microbiology*, 16(11), 528-34. doi:10.1016/j.tim.2008.08.006
- Ramon-Garcia, S., Gonzalez Del Rio, R., Villarejo, A. S., Sweet, G. D., Cunningham, F., Barros, D., Thompson, C. J. (2016). Repurposing clinically approved cephalosporins for tuberculosis therapy. *Sci Rep*, 6, 34293. doi:10.1038/srep34293
- Reported Tuberculosis in the United States. (2007). In Atlanta, GA: CDC.
- Rodrigues-Junior, V. S., Villela, A. D., Goncalves, R. S., Abadi, B. L., Trindade, R. V., Lopez-Gavin, A., Santos, D. S. (2016). Mefloquine and its oxazolidine derivative compound are active against drug-resistant Mycobacterium tuberculosis strains and in a murine model of tuberculosis infection. *Int J Antimicrob Agents*, 48(2), 203-207. doi:10.1016/j.ijantimicag.2016.04.029
- Ryndak, M., Wang, S., & Smith, I. (2008). PhoP, a key player in Mycobacterium tuberculosis virulence. *Trends in Microbiology*, 16(11), 528-534. doi:<http://dx.doi.org/10.1016/j.tim.2008.08.006>

- Santos-Beneit, F. (2015). The Pho regulon: a huge regulatory network in bacteria. *Frontiers in Microbiology*, 6, 402. <http://doi.org/10.3389/fmicb.2015.00402>
- Sayes, F., Sun, L., Di Luca, M., Simeone, R., Degaiffier, N., Fiette, L., Majlessi, L. (2012). Strong immunogenicity and cross-reactivity of Mycobacterium tuberculosis ESX-5 type VII secretion: encoded PE-PPE proteins predicts vaccine potential. *Cell Host Microbe*, 11(4), 352-363. doi:10.1016/j.chom.2012.03.003
- Schluger, N. W., & Rom, W. N. (1988). The host immune response to tuberculosis. *American Journal of Respiratory and Critical Care Medicine*, 157, 679-691.
- Shah, S., & Briken, V. (2016). Modular Organization of the ESX-5 Secretion System in Mycobacterium tuberculosis. *Front Cell Infect Microbiol*, 6, 49. doi:10.3389/fcimb.2016.00049
- Simeone, R., Bobard, A., Lippmann, J., Bitter, W., Majlessi, L., Brosch, R., & Enninga, J. (2012). Phagosomal rupture by Mycobacterium tuberculosis results in toxicity and host cell death. *PLoS Pathog*, 8(2), e1002507. doi:10.1371/journal.ppat.1002507
- Simeone, R., Bottai, D., & Brosch, R. (2009). ESX/type VII secretion systems and their role in host-pathogen interaction. *Curr Opin Microbiol*, 12(1), 4-10. doi:10.1016/j.mib.2008.11.003
- Simons, F. E. R. (1989). H1-receptor antagonists: Clinical pharmacology and therapeutics. *Journal of Allergy and Clinical Immunology*, 84(6), 845-861. doi:http://dx.doi.org/10.1016/0091-6749(89)90377-1
- Singh, A., Mai, D., Kumar, A., & Steyn, A. J. (2006). Dissecting virulence pathways of Mycobacterium tuberculosis through protein-protein association. *Proc Natl Acad Sci U S A*, 103(30), 11346-11351. doi:10.1073/pnas.0602817103
- Smith, I. Mycobacterium tuberculosis pathogenesis and molecular determinants of virulence.



- Solomonson, M., Setiাপutra, D., Makepeace, K.A., Lameignere E., Petrotchenko, E.V., Conrady, D.G., Bergeron, J.R., Vuckovic, M., DiMaio, F., Borchers, C.H., Yip, C.K. Strynadka, M.C. (2015). Structure of espB from the eSX-1 type VII secretion system and insights into its export mechanism. *Structure (London, England: 1993)*, 23(3), 571-83. doi:10.1016/j.str.2015.01.002
- Stanley, S. A., & Cox, J. S. (2013). Host-pathogen interactions during Mycobacterium tuberculosis infections. *Curr Top Microbiol Immunol*, 374, 211-241. doi:10.1007/82\_2013\_332
- Stanley, S.A., Raghavan, S., Hwang, W.W., Cox, J.S. (2003). Acute infection and macrophage subversion by Mycobacterium tuberculosis require a specialized secretion system. *Proceedings of the National Academy of Sciences*, 100, 13001-13006. doi:10.1073/pnas.2235593100
- Stock, A. M., Robinson, V. L., & Goudreau, P. N. (2000). Two-component signal transduction. *Annual review of biochemistry*, 69(1), 183-215.
- Stoop, E. J., Bitter, W., & van der Sar, A. M. (2012). Tubercle bacilli rely on a type VII army for pathogenicity. *Trends Microbiol*, 20(10), 477-484. doi:10.1016/j.tim.2012.07.001
- Takenaka, K., Yoshida, K., Nishizaki, T., Korenaga, D., Hiroshige, K., Ikeda, T., & Sugimachi, K. (1995). Postoperative prophylactic lipiodolization reduces the intrahepatic recurrence of hepatocellular carcinoma. *The American journal of surgery*, 169(4), 400-405.
- Tiwari, B. M., Kannan, N., Vemu, L., & Raghunand, T. R. (2012). The Mycobacterium tuberculosis PE proteins Rv0285 and Rv1386 modulate innate immunity and mediate bacillary survival in macrophages. *PLoS One*, 7(12), e51686. doi:10.1371/journal.pone.0051686
- Tortoli, E. (2014). Microbiological features and clinical relevance of new species of the genus Mycobacterium. *Clinical microbiology reviews*, 27(4), 727-752.
- Tuberculosis (TB). (n.d.). Retrieved April 30, 2017, from <http://www.who.int/mediacentre/factsheets/fs104/en/>

- Velmurugan, K., Chen, B., Miller, J. L., Azogue, S., Gurses, S., Hsu, T., Briken, V. (2007). Mycobacterium tuberculosis nuoG is a virulence gene that inhibits apoptosis of infected host cells. *PLoS Pathog*, 3(7), e110. doi:10.1371/journal.ppat.0030110
- Verma, G., Chuck, A. W., & Jacobs, P. (2013). Tuberculosis screening for long-term care: a cost-effectiveness analysis. *Int J Tuberc Lung Dis*, 17(9), 1170-1177. doi:10.5588/ijtld.12.0934
- Wagner, J. M., Chan, S., Evans, T. J., Kahng, S., Kim, J., Arbing, M. A., Korotkov, K. V. (2016). Structures of EccB1 and EccD1 from the core complex of the mycobacterial ESX-1 type VII secretion system. *BMC Struct Biol*, 16, 5. doi:10.1186/s12900-016-0056-6
- Walters, S. B., Dubnau, E., Kolesnikova, I., Laval, F., Daffe, M., & Smith, I. (2006). The Mycobacterium tuberculosis PhoPR two-component system regulates genes essential for virulence and complex lipid biosynthesis. *Molecular Microbiology*, 60(2), 312-330. doi:10.1111/j.1365-2958.2006.05102.x
- Weerdenburg, E. M., Abdallah, A. M., Mitra, S., de Punder, K., van der Wel, N. N., Bird, S., van der Sar, A. M. (2012). ESX-5-deficient Mycobacterium marinum is hypervirulent in adult zebrafish. *Cell Microbiol*, 14(5), 728-739. doi:10.1111/j.1462-5822.2012.01755.x
- Wirth, S. E., Krywy, J. A., Aldridge, B. B., Fortune, S. M., Fernandez-Suarez, M., Gray, T. A., & Derbyshire, K. M. (2012). Polar assembly and scaffolding proteins of the virulence-associated ESX-1 secretory apparatus in mycobacteria. *Mol Microbiol*, 83(3), 654-664. doi:10.1111/j.1365-2958.2011.07958.x
- Wu, X., Zhang, J., He, X., Wang, C., Lian, L., Liu, H., Lan, P. (2012). Postoperative adjuvant chemotherapy for stage II colorectal cancer: a systematic review of 12 randomized controlled trials. *J Gastrointest Surg*, 16(3), 646-655. doi:10.1007/s11605-011-1682-8

Yerushalmy, J., & Milkovich, L. (1965). Evaluation of the teratogenic effect of meclizine in man.

*American Journal of Obstetrics and Gynecology*, 93(4), 553-562.

doi:[http://dx.doi.org/10.1016/0002-9378\(65\)90515-6](http://dx.doi.org/10.1016/0002-9378(65)90515-6)

Zumla, A., Nahid, P., & Cole, S. T. (2013). Advances in the development of new tuberculosis drugs and treatment regimens. *Nat Rev Drug Discov*, 12(5), 388-404. doi:10.1038/nrd4001